



# LUND UNIVERSITY

## Molecular Recognition Materials Synthesized Based on Small molecules, DNA, and Imprinted Polymers for Bioanalytical Applications

Xue, Xiaoting

2023

[Link to publication](#)

*Citation for published version (APA):*

Xue, X. (2023). *Molecular Recognition Materials Synthesized Based on Small molecules, DNA, and Imprinted Polymers for Bioanalytical Applications*. Department of Chemistry, Lund University.

*Total number of authors:*

1

### General rights

Unless other specific re-use rights are stated the following general rights apply:

Copyright and moral rights for the publications made accessible in the public portal are retained by the authors and/or other copyright owners and it is a condition of accessing publications that users recognise and abide by the legal requirements associated with these rights.

- Users may download and print one copy of any publication from the public portal for the purpose of private study or research.
- You may not further distribute the material or use it for any profit-making activity or commercial gain
- You may freely distribute the URL identifying the publication in the public portal

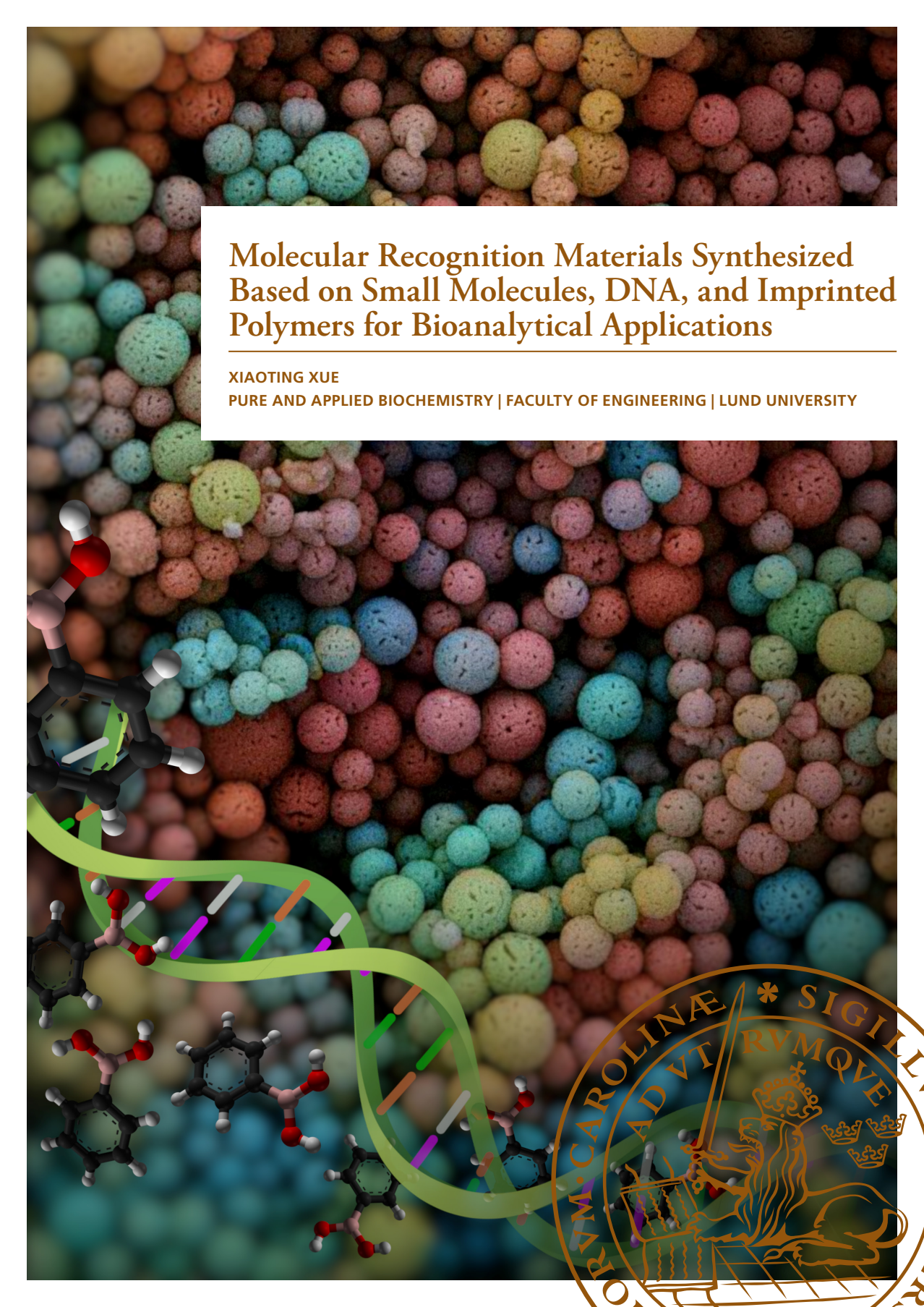
Read more about Creative commons licenses: <https://creativecommons.org/licenses/>

### Take down policy

If you believe that this document breaches copyright please contact us providing details, and we will remove access to the work immediately and investigate your claim.

LUND UNIVERSITY

PO Box 117  
221 00 Lund  
+46 46-222 00 00



# Molecular Recognition Materials Synthesized Based on Small Molecules, DNA, and Imprinted Polymers for Bioanalytical Applications

XIAOTING XUE

PURE AND APPLIED BIOCHEMISTRY | FACULTY OF ENGINEERING | LUND UNIVERSITY



Four years of study, like seasons so fond,  
in the end, a chapter learning beyond.

Molecular Recognition Materials Synthesized Based on Small molecules,  
DNA, and Imprinted Polymers for Bioanalytical Applications



# Molecular Recognition Materials Synthesized Based on Small Molecules, DNA, and Imprinted Polymers for Bioanalytical Applications

Xiaoting Xue



**LUND**  
UNIVERSITY

## DOCTORAL DISSERTATION

Doctoral dissertation for the degree of Doctor of Philosophy (PhD) at the Faculty of Engineering at Lund University to be publicly defended on 12th of December at 09.00 in B Hall, Department of chemistry, Naturvetarvägen 14, Lund

*Faculty opponent*

Professor Peter Cormack

Department of Pure & Applied Chemistry, University of Strathclyde, UK.

**Organization:** LUND UNIVERSITY  
Division of Pure and Applied Biochemistry  
P.O.Box 124  
SE-221 00 Lund, Sweden

**Document name:** DOCTORAL DISSERTATION  
**Date of issue:** 2023-12-12

**Sponsoring organization:** CSC, VR

**Author(s):** Xiaoting Xue

**Title and subtitle:** Molecular Recognition Materials Synthesized Based on Small Molecules, DNA, and Imprinted Polymers for Bioanalytical Applications

**Abstract:**

The development of sensitive, convenient, and cost-effective methods for detecting disease biomarkers is very important for meeting the growing demand for early clinical diagnosis. Additionally, the detection of disease biomarkers at ultralow concentrations is very important for disease prevention and treatment and posttreatment rehabilitation. However, current ultrasensitive detection strategies often require sophisticated instruments or complex sample pretreatments that may not be available in laboratories that have limited resources. Therefore we focused on assembling various inorganic and organic building blocks to synthesize integrated multifunctional materials and improve the performance of analytical systems and methods.

Boronic acid (BA), which is a small synthetic molecule, was conjugated in nanopores of dendritic fibrous nanosilica (DFNS) through a high-efficiency click reaction and a temperature-responsive polymer intermediate. The developed boronate affinity materials provide more affinity sites for *cis*-diol enrichment, and the well-defined narrow pores of DFNS provide highly selective affinity binding toward low-molecular-weight *cis*-diols. Moreover, a BA derivative, 4-vinylphenylboronic acid (VPBA), was employed to develop a fluorescence technique for monitoring molecular imprinting in real time and gaining insights into molecular recognition mechanisms. Molecularly imprinted polymers (MIPs) were synthesized using Alizarin Red S (ARS) as the template and VPBA as the functional monomer. The fluorogenic VPBA-ARS complex enables molecular imprinting signaling. The resulting MIPs also exhibited specific binding toward ARS and served as a fluorescent probe for detecting Cu<sup>2+</sup> ions without any tedious sample preparation.

Fluorescein-labeled single-stranded nucleic acid was directly adsorbed on polydopamine-functionalized DFNS to develop a "turn-on" fluorescence biosensor, which functions using an adsorption-quenching-recovery mechanism that enables the simple and highly efficient detection of nucleic acid biomarkers. A proof of concept was demonstrated using microRNA as a biomarker model.

Nucleic acid amplification and MIPs were employed to achieve the low-cost, simple, and reliable detection and quantification of protein biomarkers. MIPs were prepared using Pickering emulsion polymerization and DFNS as a stabilizer to produce surface-accessible binding sites for protein biomarkers. The MIPs-induced protein recognition was amplified by the hybridization chain reaction and translated into an easily detectable fluorescence signal.

**Key words:** detection, molecularly imprinted polymers, boronic acid, DNA, dendritic fibrous nanosilica

Classification system and/or index terms (if any)

Supplementary bibliographical information

**Language:** English

**ISSN and key title:**

**ISBN** 978-91-8096-002-1(print)

**ISBN** 978-91-8096-003-8(digital)

Recipient's notes

**Number of pages:** 168

Price

Security classification

I, the undersigned, being the copyright owner of the abstract of the above-mentioned dissertation, hereby grant to all reference sources permission to publish and disseminate the abstract of the above-mentioned dissertation.

Signature

Date 2023-11-01

# Molecular Recognition Materials Synthesized Based on Small Molecules, DNA, and Imprinted Polymers for Bioanalytical Applications

Xiaoting Xue



**LUND**  
UNIVERSITY

Coverphoto by Xiaoting Xue

Copyright pp 1-52 Xiaoting Xue

Paper 1 © the Authors (Open Access)

Paper 2 © the Authors (Open Access)

Paper 3 © the Authors (Manuscript unpublished)

Paper 4 © the Authors (Open Access)

Faculty of Engineering

Department of Chemistry

Division of Pure and Applied Biochemistry

ISBN 978-91-8096-002-1(print)


ISBN 978-91-8096-003-8(digital)

Printed in Sweden by Media-Tryck, Lund University

Lund 2023



Media-Tryck is a Nordic Swan Ecolabel  
certified provider of printed material.  
Read more about our environmental  
work at [www.mediatryck.lu.se](http://www.mediatryck.lu.se)

**MADE IN SWEDEN** 

*To my family*

# Table of Contents

Popular science summary .....	1
Populärvetenskaplig sammanfattning.....	3
论文简介 .....	5
Abstract .....	7
List of Papers.....	8
My contributions to the papers .....	9
Abbreviations .....	10
<b>Chapter 1 Introduction .....</b>	<b>12</b>
1.1 Background .....	12
1.2 Aim and scope of this thesis.....	13
<b>Chapter 2 Boronic acid-enabled molecular recognition and signaling.....</b>	<b>15</b>
2.1 Boronic acid reactivity .....	15
2.2 Boronate affinity materials .....	16
2.2.1 Dendritic fibrous silica nanoparticles .....	16
2.2.2 Polymer brushes .....	18
2.2.3 Boronic acid functionalized DFNS.....	19
2.3 Fluorescent probes for boronic acids.....	21
2.3.1 Alizarin Red S .....	21
2.3.2 Boronic acid–alizarin complex incorporated nanoparticles .....	23
<b>Chapter 3 Nucleic acid signal amplification and sensing.....</b>	<b>25</b>
3.1 Nucleic acid hybridization .....	25
3.1.1 DNA hairpins.....	25
3.1.2 Hybridization chain reaction .....	26
3.2 Functional nucleic acids .....	27
3.3 Nucleic acid-functionalized DFNS .....	29
<b>Chapter 4 Molecularly imprinted polymers .....</b>	<b>32</b>
4.1 Noncovalent imprinting.....	32
4.2 Covalent imprinting based on boronate affinity .....	34
4.3 DNA in molecular imprinting and sensing.....	37

<b>Chapter 5 Conclusion and future outlooks .....</b>	<b>39</b>
<b>Acknowledgements .....</b>	<b>41</b>
<b>References .....</b>	<b>43</b>



## Popular science summary

In the modern world, many different natural and man-made substances are everywhere, from the air we breathe to the food we eat. To protect public safety and health, the ability to analyze these substances is crucial. In medicine, for instance, the rapid and accurate detection of molecules can help diagnose diseases early. For example, during the COVID-19 pandemic, rapid antigen tests were essential to determine if someone had the virus. Do you know how these tests work?

A typical rapid antigen test device is contained in a plastic box marked with “S” (sample holder), “T” (test) and “C” (control). To detect the virus, three types of antibodies work together in rapid antigen test: gold-labeled, and T- and C-line fixed antibodies, denoted as “E”, “F” and “G”, respectively. At the “S” spot, “E” reaches out and grabs a specific part of the virus if it is present in the sample. As the sample flows to the “T” area, “F” reaches out and grabs the virus that was previously grabbed by “E” and locks it into the “T” area. The gold nanoparticles attached on “E” appear as a line in the “T” area. Any extra “E” that does not catch the virus continues to flow to the “C” area. In the C area, the extra “E” (together with the attached gold nanoparticles) is captured by the fixed “G” to generate a second line, indicating that the test is working properly. These antibodies play a crucial role in the antigen test, and they work in a way like how different locks fit perfectly their corresponding keys. With the help of the gold nanoparticles, the detection of virus is achieved with naked eye.

To produce a detection kit or device, although antibodies are often the first choice, the direct use of antibodies is somewhat problematic. First, antibodies do not last very long, and they are not very stable, especially outside of their natural environments. Additionally, because the acquisition of antibodies can be expensive, time-consuming, and laborious, finding more durable and reliable substitutes that have functionalities similar to those of antibodies is very important.

In this thesis, we explore a group of special materials called “molecular recognition materials” which are chemically designed to have the right shapes and structures to bind specific targets with sufficient strength. In this thesis, two strategies are investigated for synthesizing molecular recognition materials.

One approach involves chemically combining molecular building blocks with emerging nanomaterials. Boronic acid is a building block that can catch molecules that have certain structures, such as sugars. Single-stranded DNA is another building block that can fit together with complementary single-stranded DNA. This means if the target is a particular single-stranded DNA, a complementary single-stranded DNA can be used to catch the target through base matching. To enhance the ability of these building blocks for catching targets, they are combined with porous silica particles. The porous silica particles can offer a large surface area and well-controlled pore sizes to improve molecular detection and quantification.

The second approach involves the use of molecularly imprinted polymers (MIPs), which are often referred to as “artificial receptors” or “plastic antibodies.” MIPs are polymers that are specially designed against a specific target. By molecular imprinting, specific binding sites are created in crosslinked polymers. This process is similar to pressing a modelling clay with your thumb, which leaves a unique fingerprint of your thumb on the clay.

Once these molecular recognition materials are established, the challenge is to convert the event of molecular binding to a detectable signal. In the rapid antigen test, the capture of virus by the antibody causes aggregation of the gold nanoparticles, which indicates the presence of the virus in the sample. In this thesis, fluorescent molecules were employed as signaling tools. When a target molecule attaches to the molecular recognition material, it activates or deactivates fluorescent molecules, which strengthens or weakens the fluorescence signal. This can be measured using specialized equipment, such as a fluorescence spectrometer, to provide valuable information about the presence and concentration of the target molecule.

## Populärvetenskaplig sammanfattning

I vår moderna värld omges vi av olika naturliga och konstgjorda ämnen. Dessa finns överallt - i luften vi andas och maten vi äter. Det är viktigt att analysera dem för vår säkerhet och hälsa. I medicinfältet kan snabb och korrekt detektion av molekyler hjälpa till att tidigt diagnostisera sjukdomar. Till exempel, under COVID-19-pandemin var snabba tester kallade antigen-snabbtester avgörande för att fastställa om någon hade viruset. Vet du hur dessa tester fungerar?

Ett typisk antigen-snabbtest är en plastlåda märkt med S (sample), T (test) och C (control). Det finns tre typer av antikroppar som samverkar i antigen-snabbtestet för detektering, de är antikroppar med nanopartiklar i guld, antikroppar som är fixerade vid T-linjen och antikroppar som är fixerade vid C-linjen, vi kallar de tre antikropparna för E, F och G, respektive. På S fångar E en specifik del av COVID-viruset om de finns i provet. Provet flyter sedan upp genom testområdet med hjälp av kapillärkraften. Vid T sträcker F ut sig och fångar COVID-virus som redan har fångats av E och låser fast dem på plats. Guldnanopartiklarna kommer sedan synas som en linje på testet. Eventuell överbliven E som inte fångade något virus fortsätter upp till C-linjen där en liknande process äger rum, men här fångas alla E av G som skapar en annan linje i C-området som indikerar att testet fungerar som tänkt. Dessa antikroppar spelar en avgörande roll i antigen-testet. De fungerar som små lås som låser sig fast på viruset, och med hjälp av guldnanopartiklarna gör de viruset synligt.

Antikroppar är en central del i dessa tester men det finns vissa problem med att använda antikroppar. För det första är de instabila och håller inte särskilt länge, särskilt utanför naturliga miljöer. För det andra är det dyrt och tidskrävande att skapa antikroppar. Dessa problem gör det viktigt att hitta mer hållbara och pålitliga substitut.

Detta examensarbete går ut på att utforska smarta material som kallas "recognition materials". Dessa material är kemiskt utformade med specifika former och strukturer för att starkt binda till specifika mål molekyler precis som antikroppar. Examensarbetet innefattar två strategier för att skapa dessa "recognition materials".

Ett tillvägagångssätt är att kemiskt kombinera molekyllära byggstenar med nya typer av nanomaterial. Boronsyra är en typ av byggsten som kan fånga molekyler med vissa strukturer, som socker. Enkelsträngad DNA är en annan byggsten som kan binda med komplementär enkelsträngad DNA. Detta innebär att om din mål molekyl är en specifik enkelsträngad DNA kan du designa en komplementär enkelsträngad DNA för att fånga den. För att göra dessa byggstenar ännu bättre på att fånga mål molekyler täcker man nanopartiklar av poröst kisel med dessa molekyllära byggstenar, vilket ökar ytarean och kan erbjuda storleksselektion.

Det andra tillvägagångssättet innefattar användningen av molekyllära avtryck (MIP), som ofta kallas "konstgjorda antikroppar" eller "antikroppar i plast". MIP är

speciellt utformade polymerer som formas runt en specifik målmolekyl. Denna process kan liknas vid att forma modellera runt din tumme, vilket lämnar ett unikt avtryck i leran av din tumme.

När dessa “recognition materials” väl har fångat sina målmolekyler ligger nästa utmaning i att omvandla denna händelse till en detekterbar signal. I fallet med antigen-snabbtesterna leder fångsten av viruset till en aggregering av guldnanopartiklarna, vilket leder till en färgförändring som visar att viruset finns. I detta examensarbete används fluorescerande molekyler som signalverktyg. När en målmolekyl fäster sig vid en MIP aktiverar eller inaktiverar målmolekylen de fluorescerande molekylerna, vilket resulterar i en starkare eller svagare fluorescerande signal. Denna signalintensitet kan mätas med specialutrustning (fluorescensspektrometri) och ger värdefull information om närvaron och koncentrationen av målmolekylen.

# 论文简介

在现代社会，我们周围存在着各种各样肉眼所看不见的东西。这里面有自然界产生的，也有人工制造的各种大大小小的分子。从我们呼吸的空气到我们吃的食物，它们几乎无处不在。为了确保我们的健康和安全，我们必须能够检测并分析某些特定的分子。特别是在医学领域，快速而准确地检测与疾病相关的分子标记物可以帮助我们早期就能发现病原并尽快进行治疗。例如在 COVID-19 疫情中，抗原快速检测可以迅速判断某人是否感染了病毒。那么，你知道这样的快速检测是如何实现的吗？

抗原快速检测实际上是通过一个简易的塑料盒完成的。在这个塑料盒里，三种不同抗体（为方便起见我们分别将这三个抗体命名为 E、F 和 G）被放置在三个不同的区域，称为 S(样本)、T(测试)和 C(控制)区。放置在 S 区的抗体 E 被标记了金纳米颗粒，它可以通过毛细管作用流向 T 区和 C 区。在 T 区的抗体 F 和在 C 区的抗体 G 是被固定在载体表面而无法流动的。具体的检测过程如下：在待检样品加入 S 区以后，S 区内的抗体 E 会与样品里的病毒颗粒结合，并通过毛细管作用流到 T 区。固定在 T 区的抗体 F 能够“抓住”病毒颗粒，从而将结合在病毒颗粒上的抗体 E 保留在 T 区。这样，标记在抗体 E 上的金纳米颗粒会在测试盒中的 T 区产生一条横线，表明样品里存在有病毒颗粒。同时，没有“抓住”病毒的抗体 E 会继续流动到 C 区。固定在 C 区的抗体 G 能够识别并绑定抗体 E，从而在 C 区形成一条新的金纳米颗粒横线。这最后一条横线是用来确认通过毛细管作用驱动的液流能够正常工作。如果把抗体 E 和 F 比作两把小锁，那么我们所要检测的病毒颗粒表面上就会有相对应的两把钥匙。

显而易见，检测方法和试剂盒的开发非常依赖于高质量的抗体。尽管抗体有其独特的优点，但其寿命有限，并且在非自然环境中不太稳定。此外，抗体的生产过程既昂贵又耗时，需要投入大量的人力和物力。因此，我们需要寻找抗体的替代品。这些替代品需要具备与抗体类似的目标识别能力但有更高的稳定性，又要易于进行大规模生产和制备。

本论文的主要目标是运用化学方法制备能够替代抗体的多功能分子识别材料。这些材料不仅能够识别特定的目标分子，而且由于采用了化学合成的方法，此类材料还具有很强的稳定性并易于生产。制备分子识别材料的一种方法是通过将具有分子识别能力的小分子或大分子结合到多孔性纳米材料上来实现。例如，如果目标分析物是单链 DNA，可以通过设计一条与其互补的单链 DNA 来捕获目标 DNA。硼酸是一种能够捕捉糖分子的小分子化合物。通过将硼酸或单链 DNA 组装在多孔二氧化硅的表面，我们可以充分利用多孔二氧化硅突出的接触面积和孔径来增强硼酸和单链 DNA 的分子识别性能。另一种制备分子识别材料的方法是利用分子印迹聚合物，通常被称为“人工受体”或“塑料抗体”。分子印迹聚合物是一种经过精心设计的高分子材料，其三维结构中含有围绕特定目标分子构建的分子识别位点。分子印迹过程可以类比用大拇指按压橡皮泥。拇指按压以后，拇指指纹就被留在了橡皮泥的表面。

有了合适的分子识别材料，如何将分子识别的结果转化为可以检测的信号呢？在上面提到的抗原快速检测的例子中，抗体与病毒的结合导致金纳米颗粒聚集在 T 区形

成一条肉眼可见的横线。这条 T 区的横线显示病毒的存在。在本论文中，荧光分子被用来起到类似于金纳米颗粒的作用，从而实现有效的信号传导。当目标分子和分子识别材料结合时，这个过程会激活或猝灭荧光，从而改变系统的光学信号。通过用特定的仪器来测量信号强度，我们可以准确地探测目标分子和得知目标分子的浓度。

## Abstract

The development of sensitive, convenient, and cost-effective methods for detecting disease biomarkers is very important for meeting the growing demand for early clinical diagnosis. Additionally, the detection of disease biomarkers at ultralow concentrations is very important for disease prevention and treatment and posttreatment rehabilitation. However, current ultrasensitive detection strategies often require sophisticated instruments or complex sample pretreatments that may not be available in laboratories that have limited resources. Therefore, we focused on assembling various inorganic and organic building blocks to synthesize integrated multifunctional materials and improve the performance of analytical systems and methods.

Boronic acid (BA), which is a small synthetic molecule, was conjugated in nanopores of dendritic fibrous nanosilica (DFNS) through a high-efficiency click reaction and a temperature-responsive polymer intermediate. The developed boronate affinity materials provide more affinity sites for *cis*-diol enrichment, and the well-defined narrow pores of DFNS provide highly selective affinity binding toward low-molecular-weight *cis*-diols. Moreover, a BA derivative, 4-vinylphenylboronic acid (VPBA), was employed to develop a fluorescence technique for monitoring molecular imprinting in real time and gaining insights into molecular recognition mechanisms. Molecularly imprinted polymers (MIPs) were synthesized using Alizarin Red S (ARS) as the template and VPBA as the functional monomer. The fluorogenic VPBA–ARS complex enables molecular imprinting signaling. The resulting MIPs also exhibited specific binding toward ARS and served as a fluorescent probe for detecting  $\text{Cu}^{2+}$  ions without any tedious sample preparation.

Fluorescein-labeled single-stranded nucleic acid was directly adsorbed on polydopamine-functionalized DFNS to develop a “turn-on” fluorescence biosensor, which functions using an adsorption–quenching–recovery mechanism that enables the simple and highly efficient detection of nucleic acid biomarkers. A proof of concept was demonstrated using microRNA as a biomarker model.

Nucleic acid amplification and MIPs were employed to achieve the low-cost, simple, and reliable detection and quantification of protein biomarkers. MIPs were prepared using Pickering emulsion polymerization and DFNS as a stabilizer to produce surface-accessible binding sites for protein biomarkers. The MIP-induced protein recognition was amplified by the hybridization chain reaction and translated into an easily detectable fluorescence signal.

## List of Papers

This thesis is based on the following scientific papers, which will be referred to in the text by their Roman numerals. The publications and manuscripts are appended at the end of the thesis.

### Paper I

Xiaoting Xue, Haiyue Gong, Hongwei Zheng, and Lei Ye, **Boronic acid functionalized nanosilica for binding guest molecules.** *ACS Applied Nano Materials*, **2021**, 4, 2866-2875

### Paper II

Xiaoting Xue, Man Zhang, Haiyue Gong, and Lei Ye, **Recyclable nanoparticles based on a boronic acid–diol complex for the real-time monitoring of imprinting, molecular recognition and copper ion detection.** *Journal of Materials Chemistry B*, **2022**, 10, 6698-6706

### Paper III

Xiaoting Xue, Helena Persson, and Lei Ye, **Polydopamine functionalized dendritic fibrous silica nanoparticles as a generic platform for nucleic acid-based biosensing.** *Manuscript*

### Paper IV

Xiaoting Xue, Man Zhang, Solmaz Hajizadeh, Per-Olof Larsson, and Lei Ye, **Amplification of molecular recognition signal on imprinted polymers using hybridization chain reaction.** *ACS Applied Polymer Materials*, **2022**, 5, 1, 680-689

Publications not included in this thesis.

### Paper I

Man Zhang, Xiaoting Xue, Haiyue Gong, Baolin Liu, & Lei Ye, **Double isothermal amplification and CRISPR-cas12a for sensitive detection of citrinin.** *ACS Food Science & Technology*, **2021**, 1(10), 1997-2005.

### Paper II

Pian Wu, Man Zhang, Xiaoting Xue, Ping Ding, Lei Ye, **Dual-amplification system based on CRISPR-Cas12a and horseradish peroxidase for colorimetric detection of microcystin-LR.** *Microchimica Acta*, **2023**, 190, 314.

# My contributions to the papers

## *Paper I*

I designed the experiments with the help of coauthors, performed all the experiments and all the experimental data analysis. I wrote the first draft of the paper and made revisions together with other coauthors.

## *Paper II*

I designed the experiments with the help of Lei Ye, performed all the experiments and all the experimental data analysis. I wrote the first draft of the paper and made revisions together with other coauthors.

## *Paper III*

I designed the experiments independently, performed all of the experiments except for miR-21 extraction from cells, and all the experimental analysis. I wrote the first draft of the paper and made revisions together with other coauthors.

## *Paper IV*

I designed the majority of the experiments, performed all of the experiments except for fluorescent microscopy experiment, and most of the experimental analysis. I wrote the first draft of the paper and made revisions together with other coauthors.

## Abbreviations

ARS	Alizarin red S
ATRP	Atom transfer radical polymerization
AuNP	Gold colloid nanoparticles
BA	Boronic acid
BAMs	Boronate affinity materials
BAs	Boronic acid and derivatives
BHQ1	Black hole quencher
CuAAC	Cu(I)-catalyzed alkyne–azide cycloaddition
DFNS	Dendritic fibrous nanosilica
dsDNA	Double-stranded DNA
ENR	Enrofloxacin
FAM	6-Carboxyfluorescein
FNAs	Functional nucleic acids
FRET	Förster resonance energy transfer
FRP	Free radical polymerization
HCR	Hybridization chain reaction
hpDNA	DNA hairpin
LCST	Lower critical solution temperature
MBs	Molecular beacons
MIPs	Molecularly imprinted polymers
PCR	Polymerase chain reaction
PDA	Polydopamine
pGMA	poly(glycidyl methacrylate)
pNIPAm	poly(N-isopropylacrylamide)
QD	Quantum dots
ROS	Reactive oxygen species
SAMs	Self-assembled monolayers

SELEX	Exponential enrichment
SNAs	Spherical nucleic acids
ssDNA	Single strand DNA
UCNPs	Upconversion nanoparticles
VPBA	4-vinylphenylboronic acid

# Chapter 1 Introduction

## 1.1 Background

Molecular recognition elements are constructed for providing selective target binding from a mixture of different (and sometimes closely related) compounds, materials, or living cells. The high specificity and affinity of molecular recognition elements are achieved by appropriate structures that enable multipoint noncovalent or covalent interactions with the target. Such highly selective binding is called “molecular recognition”.

Molecular recognition elements can range from small coordination compounds, such as crown ethers and boronic acid derivatives, to macromolecules, such as enzymes, antibodies, and nucleic acids. With the rapid development of materials science and nanotechnology, these synthetic molecular receptors and biological molecular recognition elements have been incorporated into polymer matrices or functionalized nanostructured materials to obtain molecular recognition materials. In this manner, the selectivity and sensitivity of molecular recognition elements could be enhanced. Additionally, molecular recognition materials that have functionalities of both polymers and nanomaterials are more robust for practical applications.

Boronic acid and derivatives (BAs) are highly valuable in molecular recognition owing to their unique ability to recognize *cis*-diol motifs through the formation of boronic esters. Although the reaction involves the formation of covalent bonds, it is still reversible. The binding of diols by boronic acids occurs in a bivalent manner at the molecular level. To enhance the affinity for compounds containing *cis*-diols, researchers have synthesized various dimeric derivatives of boronic acid and attached BAs to polymers and nanoparticles to develop boronic affinity materials (BAMs) that can facilitate molecular recognition for not only low-molecular-weight compounds but also macromolecules and live cells.

The complementary pairing of nucleic acid bases, which are guanine–cytosine and adenine–thymine in DNA (or guanine–cytosine and adenine–uracil in RNA), result in the formation of a double-stranded association complex (hybridization) between the formed nucleotide sequences, which is a powerful molecular recognition system. The chemical synthesis and easy modification of both DNA and RNA render them attractive candidates for integration with nanomaterials. Compared with their linear

nucleic acid counterparts, DNA- and RNA-functionalized nanomaterials have unique properties, including transfection-reagent-free uptake into cells, stronger binding affinity to their complements, minimal immunogenicity, and reduced propensity toward nuclease degradation.

Molecular imprinting involves the generation of cavities in polymer matrices that have distinct memories of template molecules. These cavities are designed to facilitate molecular recognition. Molecular imprinting relies on a combination of physical and chemical interactions between target molecules and functional monomers, which ultimately result in the formation of molecularly complementary materials or material interfaces called “molecularly imprinted polymers” (MIPs). BAs and DNA have been used as functional monomers to improve the affinity of MIPs.

To utilize molecular recognition materials for bioanalytical applications effectively, the detection and signaling of molecular recognition events must be enabled while maintaining binding affinity. In this regard, fluorescence-based signaling methods offer a promising solution, because fluorescence detection provides several advantages, including high sensitivity, selectivity, and a wide range of dynamics, which enable the detection of low concentrations of target molecules. Moreover, fluorescence detection enables multiplexing, which facilitates the simultaneous detection of multiple targets. Because it is nondestructive and noninvasive and has excellent temporal and spatial resolutions, fluorescence detection is suitable for real-time monitoring. Additionally, fluorescence detection is versatile, has a diverse range of available fluorescent dyes, and offers ease of detection and quantification.

## 1.2 Aim and scope of this thesis

The aim of this thesis is to explore different molecular building blocks to construct molecular recognition materials for bioanalytical applications. The research is focused on the assembly of multifunctional materials to improve the performance of analytical systems and methods. By combining different molecular building blocks with emerging nanomaterials, we strive to gain insights into molecular recognition mechanisms in different synthetic systems. By seeking answers to some fundamental questions underlining molecular recognition, we aim to contribute to next-generation materials that are not limited to analytical sciences but have a broader application scope.

Paper I described the immobilization of clickable BA in nanopores of dendritic fibrous nanosilica (DFNS), which was achieved using a copper-catalyzed click reaction and an optional temperature-responsive polymer brush that was synthesized *in situ*. The resulting boronate affinity material was evaluated by studying its molecular recognition characteristics for *cis*-diols using Alizarin Red S (ARS) and

nicotinamide adenine dinucleotide (NADH) as models. The impacts of the intermediate polymer and its temperature-modulated phase variation on target binding were also investigated.

Paper II introduced a fluorescence technique to enable the uninterrupted observation of dynamic interactions within the template–functional monomer complex throughout imprinting. The technique simultaneously enabled the real-time monitoring of template binding and its subsequent dissociation from the imprinted polymer. For synthesizing MIPs, 4-vinylphenylboronic acid (VPBA) and ARS were chosen as the functional monomer and template, respectively. The synthesized MIPs exhibited a strong affinity for ARS and served as an effective fluorescence sensor for detecting  $\text{Cu}^{2+}$  ions.

Paper III described the development of a simple “turn-on” fluorescence biosensor for detecting nucleic acid biomarkers. The biosensor operated through an adsorption–quenching–recovery mechanism. 6-Carboxyfluorescein-modified single-stranded DNA (FAM–ssDNA) was adsorbed on polydopamine-functionalized DFNS (DFNS@DA), which quenched the fluorescence. In the presence of a complementary target sequence, FAM–ssDNA detached from DFNS@DA, which intensified the fluorescence.

Paper IV described the development of nonenzymatic hybridization chain reaction (HCR)-amplified protein detection/quantification using MIPs as a recognition element for protein biomarkers. MIPs were prepared using Pickering emulsion polymerization (EP) and used to capture target proteins. The HCR reaction was initiated by adding ssDNA to captured proteins, followed by the addition of two hairpin DNA molecules labeled with a fluorophore and quencher. The opening of the hairpins and formation of nicked dsDNA generated fluorescence emission.

# Chapter 2 Boronic acid-enabled molecular recognition and signaling

## 2.1 Boronic acid reactivity

BA contains a trigonal planar  $sp^2$ -hybridized boron atom, which is bonded to either an alkyl or aryl group, and two hydroxyl groups. The boron center has six valence electrons (Figure 1, top left). In aqueous media, BA equilibrates between neutral hydrophobic molecules and hydrophilic hydroxyboronate anions when complexed with hydroxide ions (Figure 1, top right). When the pH is higher than the  $pK_a$ , boronate esterification is favorable. Conversely, when the pH is lower than the  $pK_a$ , hydrolysis is induced and reverses the reaction.

BAs can form esters, most frequently with 1,2- and 1,3-diols in carbohydrates, catechols, nucleosides, glycoproteins, and bacteria.<sup>1,2</sup> Initial investigations into the formation of reversible covalent bonds between boronic acids and 1,2- or 1,3-diols were reported by Lorand and Edwards, who compared covalent bond constants for different phenylboronic acids and diol compounds by observing pH drop.<sup>3</sup> Typically, when the surrounding pH is equal to or higher than the  $pK_a$  of the BAs, the BAs can form an adduct with hydroxyl groups and change to an  $sp^3$ -hybridized tetragonal boronate anion. The reaction between BAs and *cis*-diols forms five- or six-membered cyclic esters.<sup>4</sup> Conversely, when the surrounding pH is substantially lower than the  $pK_a$  value of the BAs, the BA-*cis*-diol complex dissociates because the BAs completely reverts to  $sp^2$ -hybridized trigonal configuration<sup>5,6</sup> (Figure 1, bottom). Because BAs can recognize diol motifs through boronic ester formation, they attracted considerable research attention as a functional group for targeting molecules containing *cis*-diol structures.

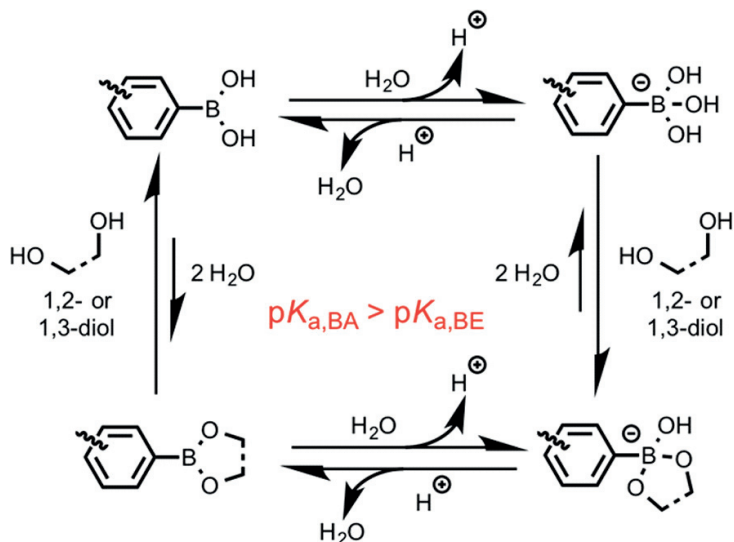


**Figure 1.** Esterification equilibrium between boronic acid or boronate anion in aqueous solution containing 1,2- or 1,3-diols, where  $pK_{a,BA}$  and  $pK_{a,BE}$  are  $pK_a$  values for boronic acid and ester, respectively. Reproduced with permission from reference 6. Copyright 2016, American Chemical Society.

## 2.2 Boronate affinity materials

With the introduction of BAs, which functions as both stimuli-responsive functional groups and targeting ligands, BAMs can selectively and reversibly bind to *cis*-diols containing compounds. Conventional BAMs have three apparent drawbacks, including non-biocompatible binding pH, weak affinity, and relatively poor selectivity, which substantially limit the practical applications of BAMs. Various BAMs, such as macroporous monoliths<sup>7-9</sup>, mesoporous materials<sup>10-11</sup>, nanoparticles<sup>12-14</sup>, MIPs<sup>15-17</sup>, and temperature-responsive materials<sup>18-19</sup>, have been developed to solve these problems.

### 2.2.1 Dendritic fibrous silica nanoparticles

In materials science, over the past few decades, extensive research has been conducted on mesoporous silica for advancing various technologies (Figure 2).<sup>20</sup> Notable contributions include the development of Mobil Composite Material (MCM-41), which contains ordered hexagonal mesopores, by Kresge and colleagues.<sup>21</sup> Similarly, Stucky et al. synthesized silica that has tunable large mesopores, known as SBA-15 (Santa Barbara, CA, USA).<sup>22</sup> In 2010, Polshettiwar

et al. introduced a simple emulsion system to generate silica-based nanospheres with dendritic fibrous characteristics.<sup>23</sup> Similarly, Du et al. utilized an ethyl ether emulsion to produce silica nanospheres, referred to as hierarchically mesoporous silica nanoparticles.<sup>24</sup> This sparked growing interest in DFNS and led to investigations on their structures and composite multifunctional properties. Notably, in 2013, Yi et al. reported the development of carbon-based DFNS by employing DFNS as templates for synthesizing mesoporous carbon.<sup>25</sup> In 2014, Chen et al. synthesized bioactive-glass-based DFNS for gene delivery applications.<sup>26</sup> Meanwhile, Zhao et al. introduced a biphasic stratification approach for fabricating three-dimensional dendritic mesoporous silica nanospheres with adjustable structures.<sup>27</sup> Additionally, in 2016, Yu et al. developed mesoporous organosilica nanoparticles that featured chemically functionalized organic and inorganic components.<sup>28</sup> Furthermore, in 2017, Polshettiwar et al. synthesized silica and titania-hybrid DFNS, which led to additional possibilities for practical application.<sup>29</sup>

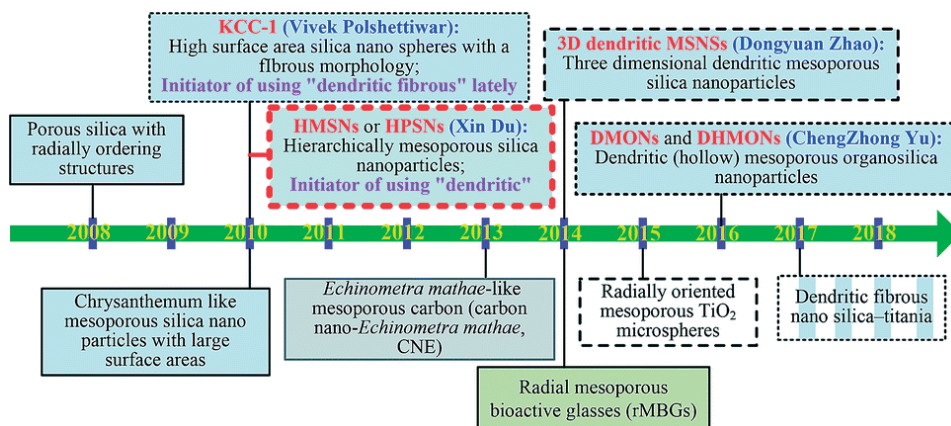


**Figure 2.** Timeline of DFNS development. Reproduced with permission from reference 20.

As shown in electron microscopy images and nitrogen adsorption isotherms (Figure 3), DFNS has a unique three-dimensional structure in which hierarchical pores are defined by numerous center-radial nanochannels. This unique architecture renders DFNS very promising for applications dependent on carrier platforms or supports. The DFNS surface and pores can be chemically modified using a postmodification or one-pot cocondensation approach, which enables the introduction of desired functional groups tailored for specific applications. Correspondingly, molecules of various sizes, such as drugs, DNA, proteins, and polymer brushes, can be loaded or coloaded *in situ* on the carrier surface and in pores by covalent conjugation, electrostatic forces, hydrophobic interactions. Consequently, DFNS-supported and

DFNS-based particles could serve as candidates for catalysis, separation, detection, energy harvesting, delivery carriers, photothermal ablation therapy, real-time imaging, etc.

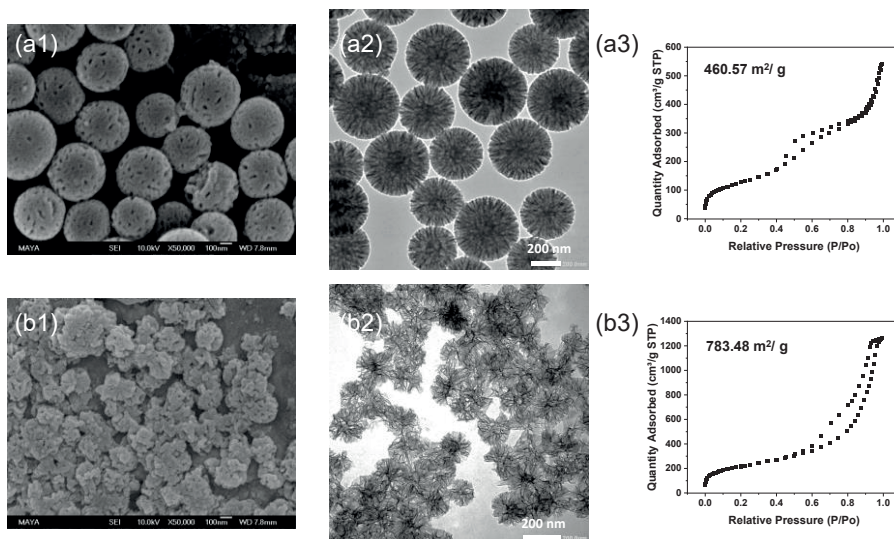


**Figure 3.** SEM images, TEM images and N<sub>2</sub> sorption isotherms of DFNS containing (a) 4 nm, (b) 20 nm pores.

## 2.2.2 Polymer brushes

Polymer brushes are dense polymer chains anchored at one end to a solid surface, to form a thin coating.<sup>30</sup> Surface-initiated controlled radical polymerizations, including atom transfer radical polymerization (ATRP), reversible addition-fragmentation chain transfer polymerization, nitroxide-mediated polymerization, and photoiniferter-mediated polymerization, are useful synthesis methods for controlling the functionality, density, and thickness of polymer brushes.<sup>31</sup> Usually, the substrate surface is first modified with an initiator monolayer, and polymer chains then directly grow from reactive sites on the immobilized initiator layer<sup>32-33</sup>(Figure 4).

Functional groups can be introduced to polymer brushes through two primary methods.<sup>34-35</sup> The first approach entails the direct surface-initiated polymerization of the corresponding monomer, which incorporates functional groups into the polymer brushes. In the second approach, functional groups can be introduced by postmodifying precursor polymer brushes, which contain appropriate reactive groups that are compatible with surface-initiated controlled radical polymerization. Figure 4 shows that the postmodification of polymer brushes can involve the modification of side-chain functional groups, such as hydroxyl, carboxylic acid,

carboxylic ester, and epoxide groups. Additionally, postmodification can be conducted at the polymer chain end, or a combination of both.

Polymer brushes are well suited for preparing various functional surfaces and endow the matrix with exquisite properties, such as corrosion protection, colloid stability,<sup>36</sup> adhesive behaviour, stimuli-responsiveness,<sup>37</sup> lubrication and friction properties, and specific molecular interactions.<sup>38</sup>

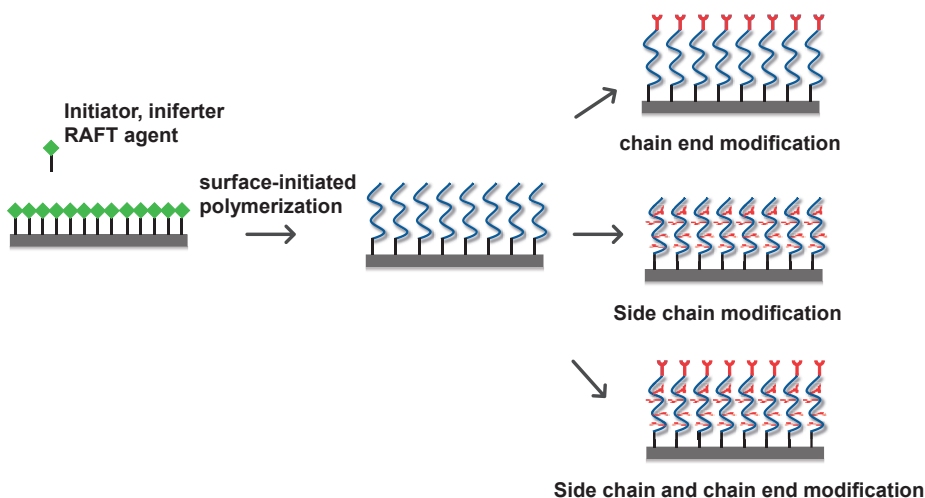


**Figure 4.** Surface-initiated polymerization and postmodification. Reproduced with permission from reference 31. Copyright 2009 American Chemical Society

### 2.2.3 Boronic acid functionalized DFNS

In Paper I, we described the investigation and use of Cu(I)-catalyzed alkyne azide cycloaddition (CuAAC) click reaction and a general-purpose polymer intermediate to immobilize boronic acid affinity ligands in DFNS nanopores. BA-functionalized DFNS were prepared by the direct click conjugation of azide-functionalized BA in alkyne-functionalized narrow pores of DFNS (Figure 5, route A) and conjugation through polymer brushes (Figure 5, route B). Thermoresponsive random polymer brushes comprising poly(N-isopropylacrylamide) (pNIPAm) and poly(glycidyl methacrylate) (pGMA) were prepared from initiator-functionalized DFNS. pNIPAm is a thermoresponsive polymer that has a characteristic lower critical solution temperature (LCST) in water at approximately 32 °C. Above the LCST, the polymer transitions from hydrophilic to hydrophobic. pGMA is widely employed for preparing functional polymer materials because its epoxy group can undergo ring-opening reactions and conjugate with azide-functionalized BA (PCAPBA) through the CuAAC click reaction.

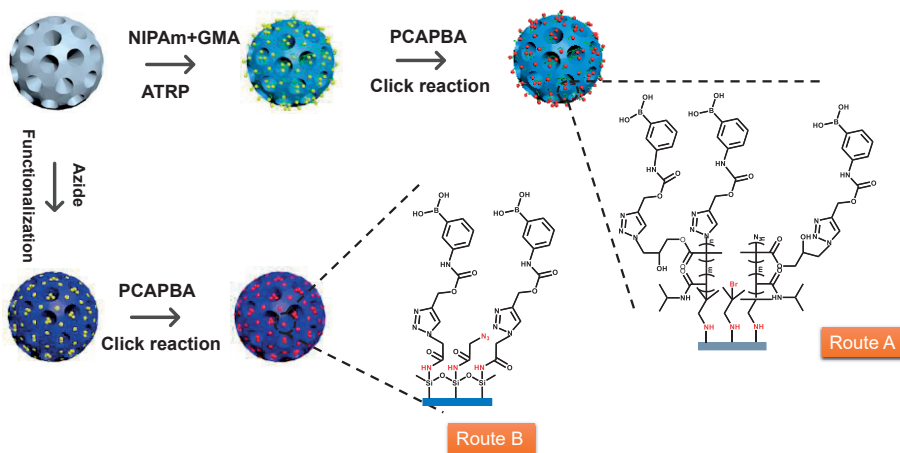


**Figure 5.** Synthesis approaches for preparing boronic acid functionalized DFNS.

Figure 6 shows that polymer-containing nanoparticles (DFNS@pco@BA) have a much higher binding capacity than polymer-free nanoparticles (DFNS@BA). By contrast, without the boronic acid ligand, the binding capacities of DFNS@N<sub>3</sub> and DFNS@pco@N<sub>3</sub> are substantially lower. The higher *cis*-diol binding capacity of DFNS@pco@BA is attributed to the higher density of boronic acid ligands immobilized on flexible polymer chains in DFNS.

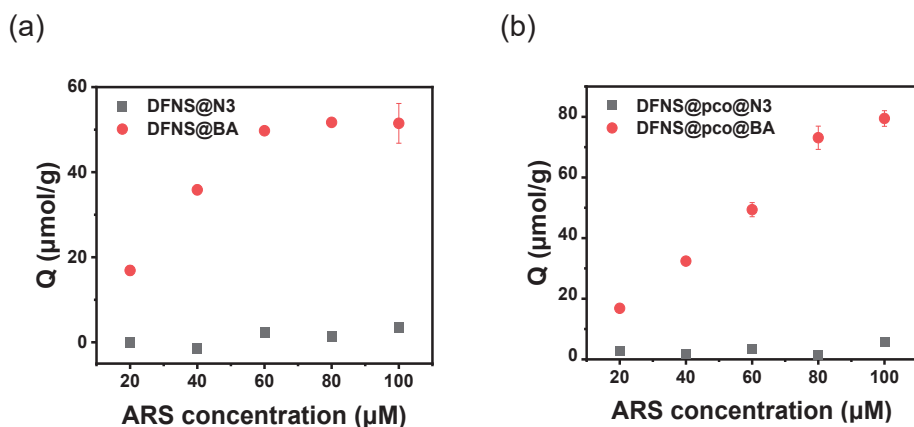


**Figure 6.** (a) ARS binding on small molecule modified DFNS (DFNS@N<sub>3</sub> and DFNS@BA) at 20 °C and pH 8.5. (b) ARS binding on polymer containing DFNS (DFNS@pco@N<sub>3</sub> and DFNS@pco@BA) at 20 °C and pH 8.5. Particle concentration was 1 mg/mL.

## 2.3 Fluorescent probes for boronic acids

### 2.3.1 Alizarin Red S

ARS dye contains diol groups. In aqueous solutions, ARS can react with BAs to form a fluorescent adduct.<sup>39-40</sup> Because the active protons in hydroxyanthraquinones are responsible for substantial fluorescence quenching,<sup>41</sup> when an ester forms from the reactions between ARS and BAs, these protons are released, which result in the absence of fluorescence quenching<sup>39, 42</sup> (Figure 7). The binding of BAs to ARS remarkably changes the fluorescence intensity and color, which render this adduct a useful fluorogenic reporter for qualitatively determining the presence of BAs.

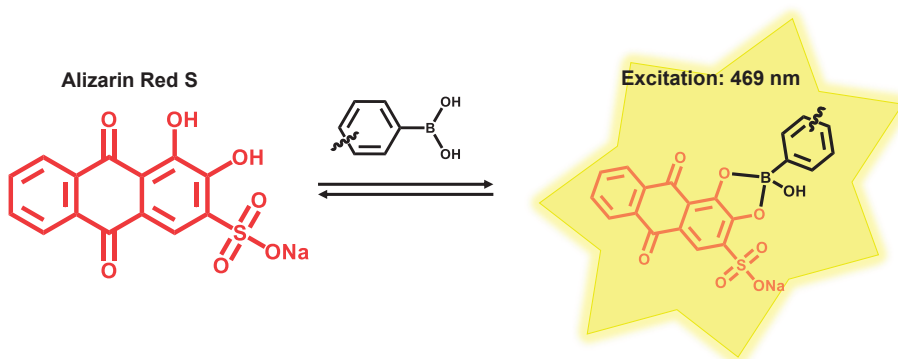


**Figure 7.** Formation of fluorescent adduct from the reaction between ARS and boronic acid.

Paper I described the use of ARS as a fluorogenic reporter to confirm that BA was introduced to both DFNS@BA and DFNS@pco@BA. As shown in Figure 8, after the ARS treatment, the spectra of DFNS@BA and DFNS@pco@BA both displayed an emission peak near 600 nm which was not observed in the spectra of DFNS@N<sub>3</sub> or DFNS@pco@N<sub>3</sub>. This result confirmed the presence of boronic acid in both boronic acid modified nanoparticles. Additionally, fluorescence emitted from DFNS@pco@BA was more intense than that emitted from DFNS@BA, which further confirmed that the boronic acid content of DFNS@pco@BA was higher than that on DFNS@BA.

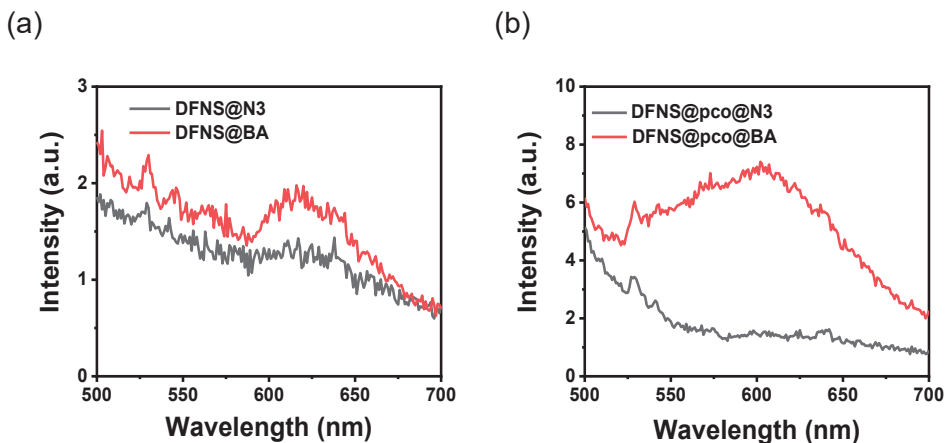


**Figure 8.** Fluorescence emissions of boronic acid modified and unmodified DFNS after mixing with ARS. (a) DFNS without polymer brush, (b) DFNS with polymer brush.

The fluorescent ARS–boronate adduct can be easily cleaved by adjusting the pH or introducing competing *cis*-diols or metal ions (Figure 9a and b). Therefore, this adduct has been extensively employed in competitive binding assays for sensing *cis*-diols-containing compounds, particularly saccharides.<sup>42</sup> Furthermore, the ARS–boronate adduct can be oxidized by reactive oxygen species (ROS) to form the corresponding phenol<sup>43</sup> (Figure 9c). ROS function as nucleophiles and coordinate with boron, and the covalent bond between the boron atom and R group is cleaved through an electronic rearrangement.<sup>44</sup> Through this mechanism, the ARS–boronate adduct has been utilized in reaction-based indicator displacement assays for sensing ROS.<sup>45–46</sup>

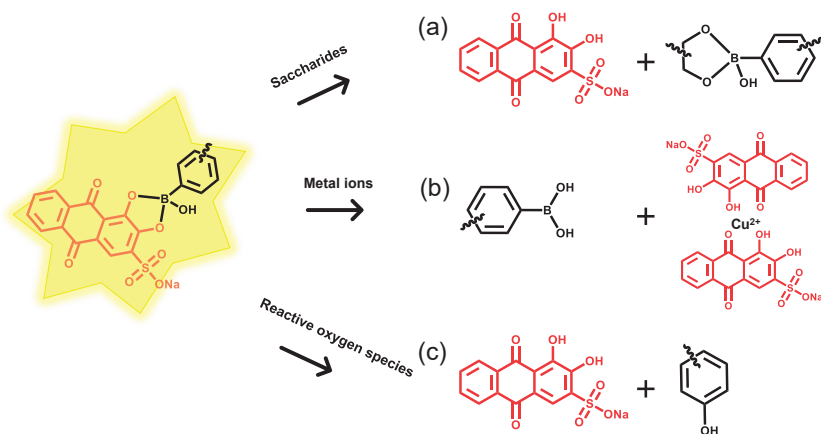


**Figure 9.** Quenching of fluorescent ARS–boronate adduct by introducing (a) saccharides, (b) metal ions, and (c) ROS.

### 2.3.2 Boronic acid–alizarin complex incorporated nanoparticles

The ARS–boronate system has been widely utilized by numerous researchers to develop fluorescence assays for detecting carbohydrates, anions, and metal ions, and considerable effort has been made to enhance the analytical performance of the ARS–boronate system in fluorescence competition assays. For instance, Li et al. demonstrated that the fluorescence of the ARS–boronate complex can be substantially intensified utilizing cationic surfactant-assembled vesicles.<sup>47</sup> Ma et al. synthesized a range of boronic acid containing acrylamide monomers, which were subsequently polymerized to polyacrylamide hydrogels. The hydrogels were loaded with ARS to produce an ARS–boronate system that exhibited colorimetric response when exposed to monosaccharides (Figure 10a).<sup>48</sup> Liang et al. developed boronic acid and ARS-functionalized poly(amidoamine) dendrimers (PAMAM). The functionalized dendrimers could discriminate between fructose, glucose, ribose, and galactose (Figure 10b).<sup>49</sup> Miao et al. designed a gold-nanocluster and ARS–boronic acid-based radiometric fluorescent probe that reliably and effectively detected glucose in rat brain microdialysate, by overcoming environmental influences (Figure 10c).<sup>50</sup>

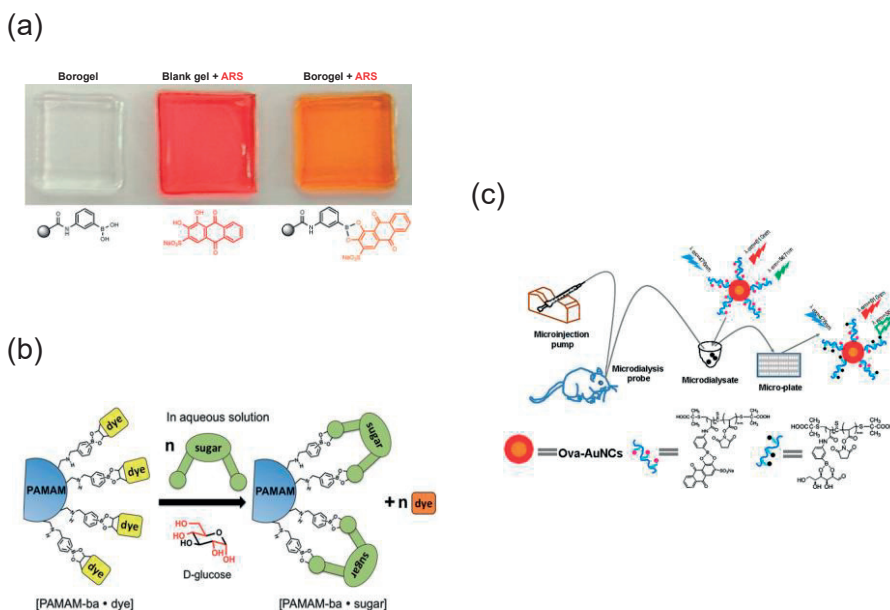


**Figure 10.** (a) Gel slabs: borogel (left), blank gel plus ARS (middle), and borogel plus ARS (right). Reprinted with permission from reference 48. (b) Sugar molecule displaces multiple dye molecules

bound to surface of the PAMAM-BA receptors in indicator displacement sensing paradigm. Reproduced with permission from Royal Society of Chemistry. (c) Principle of the fluorescent probe developed for monitoring glucose. Reprinted with permission from reference 50. Copyright 2014 American Chemical Society.

Paper II discussed how ARS MIPs that contained embedded BA groups exhibited a high affinity for ARS. These colloidal particles, to which ARS was bound, functioned as a fluorescent probe for detecting  $\text{Cu}^{2+}$  ions. When  $\text{Cu}^{2+}$  ions were present, they formed a coordination complex with ARS, which depleted ARS from MIPs and subsequently quenched the fluorescence. Figure 11a shows a linear relationship between the fluorescence intensity and the logarithm of the  $\text{Cu}^{2+}$  concentration in the range of 0.1–100 mM.

Furthermore, colloidal particles exhibited recyclability and could be used as a sensor for detecting  $\text{Cu}^{2+}$  multiple times. Because  $\text{Cu}^{2+}$  ions formed stable complexes with ARS, it caused ARS to dissociate from the MIP nanoparticles leading to quenching of fluorescence. After  $\text{Cu}^{2+}$  ions were detected, MIPs were collected and washed with an ethylenediaminetetraacetic acid solution. The obtained polymer particles were then reloaded with ARS for subsequent detection of  $\text{Cu}^{2+}$  ions. This process could be repeated multiple cycles. The ARS binding results and  $\text{Cu}^{2+}$ -induced fluorescence intensity changes in different cycles are presented in Figure 11b.

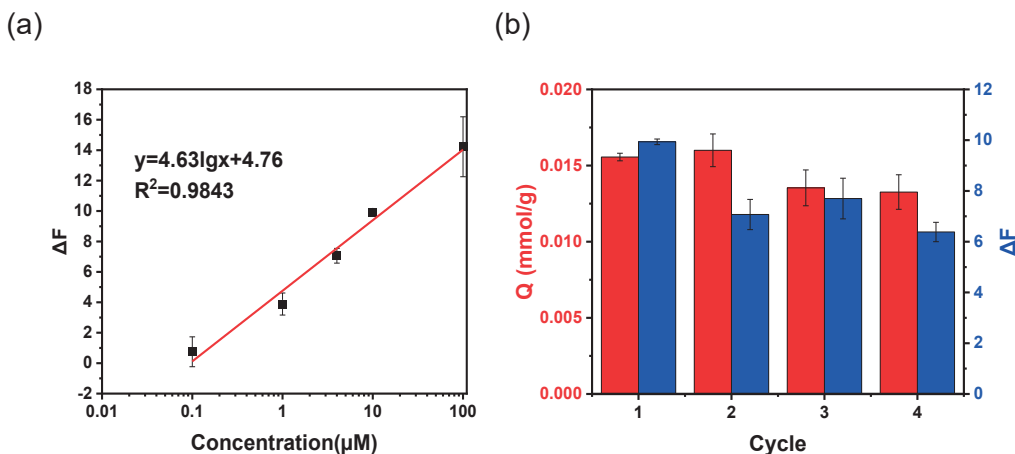


**Figure 11.** (a) Linear relationship between fluorescence intensity change and logarithm of  $\text{Cu}^{2+}$  concentration. (b) Recycling and reuse of MIP nanoparticles for adsorbing ARS and detecting  $\text{Cu}^{2+}$  in buffered solutions.

# Chapter 3 Nucleic acid signal amplification and sensing

## 3.1 Nucleic acid hybridization

The Watson–Crick hybridization of complementary sequences in nucleic acids is one of the most important fundamental processes necessary for molecular recognition *in vivo*, such as DNA replication and transcription to RNA.<sup>51–52</sup> Nucleic acid hybridization also plays a crucial role in nucleic acid identification and isolation *in vitro*, such as southern and northern blots,<sup>53</sup> the polymerase chain reaction (PCR),<sup>54</sup> and DNA sequencing.<sup>55–56</sup>

The specificity of base pairing enables perfectly complementary strands to hybridize readily and is the basis of recognition in nucleic acid sensors.<sup>57–58</sup> To achieve the selectivity required for detecting a single mismatch, researchers commonly design complementary DNA sequences to contain secondary structures or require an assembly, e.g., a hairpin structure or an assembly of multiple nucleic acid strands to recognize a single target strand.

### 3.1.1 DNA hairpins

DNA hairpins (hpDNA) are secondary structures that form when two complementary regions on the same DNA strand base-pair with one another to generate a double helix that terminates in an unpaired loop.<sup>59</sup> Compared to linear DNA, hpDNA present a higher target recognition selectivity because of their inherent structural constraint.<sup>60–61</sup>

Molecular beacons (MBs) are specifically designed hpDNA structures that are widely used as fluorescent probes.<sup>62</sup> MBs are DNA sequences that comprise one target-recognition region flanked by two short complementary stem sequences. In the absence of a target DNA or RNA, the sequence of one target-recognition region forces the entire structure to adopt a stem–loop conformation that brings the quencher and fluorophore, which are at opposite MBs ends, closer and quenches the fluorescence. In the presence of a target DNA or RNA, the target and MBs loop sequence hybridize, and the stronger intermolecular hybridization opens the weaker

stem helix. Consequently, the fluorophore and quencher spatially separate, which restores the fluorescence<sup>63-64</sup> (Figure 12a).

MBs are most commonly used for real-time PCR and other gene-detection assays.<sup>65-66</sup> MBs designed to hybridize with the forward/reverse PCR products are introduced to the PCR solution to monitor the DNA amplification of the target sequence during PCR. During annealing, more amplified target DNA molecules hybridize with MBs, which proportionally intensifies the fluorescence from the MBs. Wright et al. developed a modified molecular beacon strategy, as shown in Figure 12b, wherein hairpin DNA containing a 5' thiol and a fluorophore at the 3' end was attached to gold colloid nanoparticles (AuNP). The AuNP anchored MBs was used for imaging mRNA in live cells. When the hpDNA bound to the target RNA, the hpDNA opened and separated the fluorophore from the AuNP, which generated a fluorescence signal.<sup>67</sup>

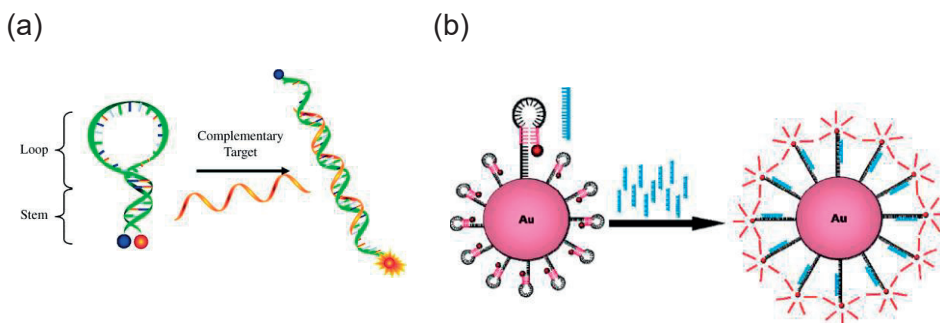


**Figure 12.** (a) Working mechanism of molecular beacon. Reprinted with permission from reference 63, Copyright 2009 WILEY-VCH Verlag GmbH & Co. KGaA, Weinheim. (b) Hairpin-DNA-functionalized gold nanoparticles used for detecting mRNA. Reprinted with permission from reference 67, Copyright 2010 American Chemical Society.

### 3.1.2 Hybridization chain reaction

HCR is a chain reaction of recognition and hybridization events between two sets of hpDNA. A target sequence (initiator) hybridizes with a hpDNA, and the hairpin structure opens and enables hybridization with a second hpDNA in a chain reaction, which yields nicked double stranded-DNA (dsDNA).<sup>68</sup> The reaction is enzyme-free and proceeds under isothermal conditions. HCR products, nicked dsDNA contain hundreds of repeating units, which provide an excellent isothermal amplification platform for detecting nucleic acid by incorporating various labels to generate signals.<sup>69</sup> HCR has been utilized for sensitively detecting a wide variety of analytes, including nucleic acids, proteins, small molecules, and cells.<sup>70</sup>

In Paper IV, HCR was designed to incorporate a fluorescence donor–acceptor into hpDNA to alter analyte-triggered fluorescence emission based on the principle of

the Förster resonance energy transfer (FRET). The principle of the HCR-based amplification and fluorescence readout is shown in Figure 13. Each hpDNA (H1 and H2) contains a stem comprising 24 base pairs enclosing a loop of 6 nucleotides (nts) and an additional sticky end comprising 6 nts (at the 5' and 3' ends of H1 and H2, respectively). The nucleotide sequences are designed to ensure that H1 and H2 form stable hairpin structures in solutions. The black hole quencher (BHQ1) and 6-carboxyfluorescein (FAM) are on the opposite sides of the stem and are brought into proximity in the hairpins. FAM has an excitation wavelength and emission peak at 484 and 518 nm, respectively. BHQ1 is a nonfluorescent azo dye that has an absorption band spanning 480–580 nm, which overlaps FAM emission and causes efficient quenching. Therefore, the H1 and H2 do not emit any fluorescence because of the FRET between FAM and BHQ1. When an initiator sequence (H0) is added, it hybridizes with H1 to form a double strand H0–H1 structure and exposes the H1 loop. The opened H1 loop then hybridizes with H2 from the sticky end, which continuously hybridizes H1 and H2, to form an extended dsDNA. The HCR changes the original hairpin structure of H1 and H2 to an extended DNA strand, which increases the distance between FAM and BHQ1 on the stem. Consequently, BHQ1 can no longer quench the FAM fluorescence.

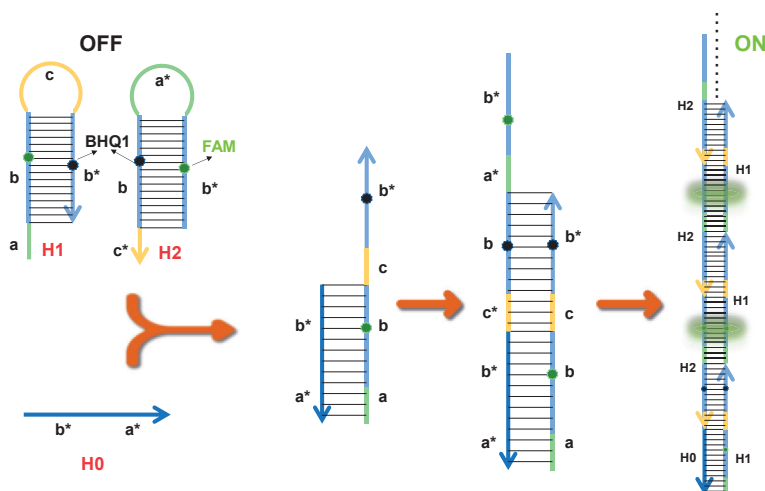


**Figure 13.** Principle of HCR-based amplification and fluorescence readout.

## 3.2 Functional nucleic acids

Nucleic acids are biomolecules that carry the most important genetic information found in Nature. Because they were discovered late relative to other biological components, considerable efforts have been made to understand their roles in the

survival and function of living systems. In addition to the role of nucleic acids for carrying genetic information, many related studies have shown that nucleic acid can be folded into different structures and that different nucleic acid sequences can perform different functions. Such nucleic acids are called “functional nucleic acids” (FANs)<sup>71-72</sup> which include aptamers, DNazymes, triplex DNA, and other unconventional nucleic acids.

Aptamers are short, synthetic, single-stranded DNA or RNA that can bind to target molecules with high specificity and affinity.<sup>73-74</sup> Typically, aptamers are generated using a selection process known as systematic evolution of ligands by exponential enrichment (SELEX),<sup>75</sup> which involves iterative cycles for incubating oligonucleotides with the desired target, partitioning unbound sequences, and subsequently recovering and amplifying bound sequences.<sup>76</sup> Over time, this process has been refined and adapted by numerous researchers to enhance its efficiency and throughput.<sup>77-78</sup> For a wide variety of molecular targets, aptamers have several advantages including high binding specificity and affinity, rapid and reliable synthesis, easy functionalization, and long-term stability.<sup>79-81</sup> These advantages enable aptamers to be promising molecular receptors for a diverse range of detecting and imaging applications.

Catalytic nucleic acids, also known as DNazymes or ribozymes, are sequence-specific nucleic acids that mimic the function of natural enzymes. Traditionally, enzymes were believed to be solely protein based. However, this perspective changed in the 1980s with the discovery of catalytic RNA called “ribozymes.”<sup>82</sup> In 1994, Breaker and Joyce further expanded this concept by developing DNazymes, which demonstrate catalytic activity by cleaving the phosphodiester linkage in RNA in the presence of Pb<sup>2+</sup> ions.<sup>83</sup> Similar to aptamers, DNazymes are usually isolated using SELEX or whole-cell-based SELEX *in vitro*. Since their discovery, a wide range of synthetic catalytic nucleic acids have been developed, including the hemin/G-quadruplex horseradish peroxidase-mimicking DNzyme,<sup>84</sup> metal-ion-dependent DNazymes,<sup>85</sup> such as Mg<sup>2+</sup>, Cu<sup>2+</sup>, Hg<sup>2+</sup>, Zn<sup>2+</sup>, Ca<sup>2+</sup>, Pb<sup>2+</sup>, and UO<sub>2</sub><sup>2+</sup>-dependent DNazymes, and cofactor-dependent DNazymes, such as histidine-dependent DNzyme<sup>86</sup>. Owing to their cofactor-dependent catalysis, DNazymes have been employed as recognition elements that can detect and report concentrations of specific cofactors.

Triplex DNA is a DNA structure that is formed through interactions between a third strand and a double-helix DNA molecule *via* Hoogsteen interactions.<sup>87-88</sup> Triplex DNA can exist in parallel or antiparallel triplex structures, depending on the specific base pairs involved, and is used as not only a recognition element<sup>89-90</sup> but also a functional structure-switching unit that enables the generation of an output signal upon target recognition.<sup>91-92</sup> Therefore, targets that can be detected using triplex DNA are not limited to specific nucleic acid sequences but cover a wide array of molecular targets, including antibodies, proteins, heavy metal ions and small molecules.

Thus, FNAs are ideal recognition elements and have been integrated with nanomaterials to enhance their targeting capabilities. Nanomaterials have several unique characteristics, including good biocompatibilities, large specific surface areas, easy surface modification and good stability.<sup>93-94</sup> FNAs can be used to functionalize nanomaterials by covalent attachment, DNA hybridization, electrostatic interactions and physical entrapment and can be easily conjugated to nanomaterials in a site-specific manner *via* various functional moieties, such as thiols, amines, carboxyl groups and biotin. The development of FNAs-functionalized nanomaterials provides more flexibility for establishing sensors that exhibit high sensitivity for molecular detection.

### 3.3 Nucleic acid-functionalized DFNS

Spherical nucleic acids (SNAs) comprise a nanoparticle core that is densely functionalized with nucleic acids. One notable advantage of three-dimensional SNAs nanostructures is that densely arranged nucleic acids have a stronger affinity with complementary target sequences than free nucleic acids *via* specific Watson–Crick base-pair hybridization. A variation of SNAs involves the adsorption of DNA on nanoparticle surfaces *via* physical interactions by functionalizing nanoparticles with PDA, which can adsorb ssDNA.

In Paper III, owing to its high surface area and V-shaped pore structure, DFNS was chosen as the core nanoparticle to prepare SNAs. After functionalizing DFNS with PDA layer, the resulting PDA-functionalized DFNS (DFNS@DA) could adsorb ssDNA to form SNAs. The FAM-labeled DNA recognition probe was absorbed on the DFNS@DA surface *via* physical interactions. Subsequently, the targets and probes were specifically bound, and rigid double-stranded structures were formed, which weakened the adsorption and binding between the DFNS@DA and the probes, and, thus, released the rigid dsDNA structures from the DFNS@DA surface. Consequently, the nucleic acid hybridization-induced desorption could be converted to a fluorescence signal (Figure 14).

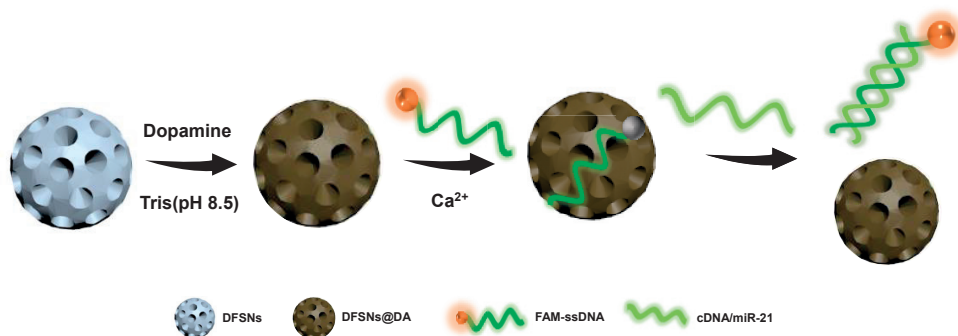


**Figure 14.** Schematic of fluorescence-switching sensing platform.

The FAM–ssDNA/DFNS@DA complex was explored for detecting miR-21, which has been identified as an important biomarker that is overexpressed in many cancers.<sup>95-96</sup> Fluorescence spectra were obtained for DFNS@DA in different concentrations of miR-21, as shown in Figure 15a. The fluorescence of the FAM–ssDNA gradually intensified with increasing miR-21 concentration from 1 to 1000 nM (Figure 15b). The fluorescence signal change ( $\Delta F$ ) linearly increased with increasing miR-21 concentration in the range from 1 to 10 nM, and the linear equation was  $\Delta F = 1.38C_{\text{miR-21}} - 1.20$  ( $R_2 = 0.9633$ ).  $\Delta F$  was linearly related to the logarithm concentration of miR-21 in the range of 10 – 1000 nM, and the linear equation was  $\Delta F = 125.02 \log C_{\text{miR-21}} - 132.8$  ( $R_2 = 0.9660$ ) and the LOD was 0.53 nM (Figure 15c and d).

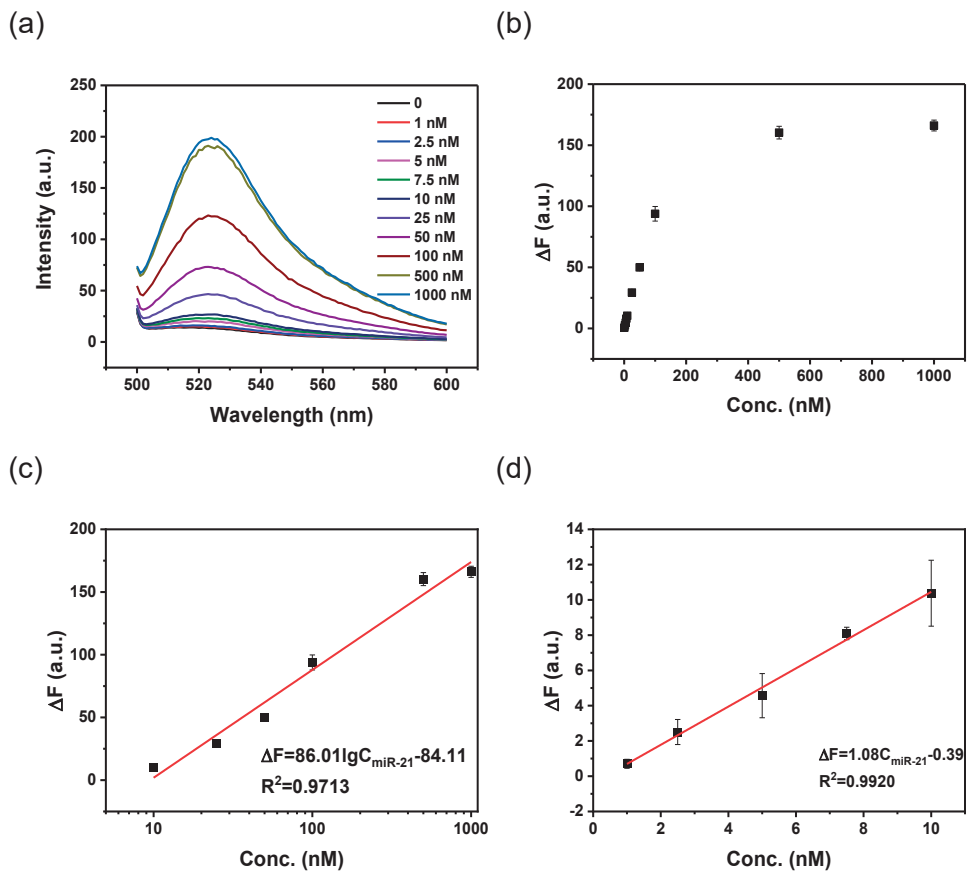


**Figure 15.** DFNS@DA performance for detecting miR-21: (a) Fluorescence spectra of FAM-ssDNA/DFNS@DA complex for detecting different concentrations miR-21. (b)  $\Delta F$  plotted as a function of miR-21 concentration. Linear correlations between  $\Delta F$  and (c)  $\log C_{\text{miR-21}}$  and (d)  $C_{\text{miR-21}}$ .

# Chapter 4 Molecularly imprinted polymers

Molecular imprinting provides an effective approach for preparing tailor-made polymer materials known as MIPs, which exhibit functionalities similar to those of antibodies and enzymes.<sup>97-98</sup> The generation of MIPs involves copolymerizing functional and crosslinking monomers in the presence of a target species that functions as a molecular template. Initially, functional monomers covalently or noncovalently form a complex with the template.<sup>99</sup> After polymerization, the highly crosslinked polymer structure holds functional monomers-template complexes in position, and the subsequent template removal produces cavities for which the size, shape, and chemical functionality complement those of templates.<sup>100-101</sup>

## 4.1 Noncovalent imprinting

Pioneered by Mosbach, noncovalent molecular imprinting only utilizes noncovalent interactions such as hydrogen bonds, ionic interactions, hydrophobic interactions, and metal-ion chelating interactions, for both molecular imprinting and subsequent rebinding.<sup>102-103</sup> Although this approach offers more flexibility for selecting functional monomers and target molecules, it may introduce some heterogeneity to binding sites owing to the presence of complexation–decomplexation equilibrium during polymerization.

To date, several synthesis strategies have been designed and developed to produce MIPs and improve the imprinting efficiency. Free radical polymerization (FRP) is the most popular method for preparing MIPs because FRP initiators have a high tolerance for a wide variety of functional monomers and can withstand different reaction conditions.<sup>104-106</sup> FRP can be triggered in different contexts, including bulk polymerization, precipitation polymerization, suspension polymerization, two-stage swelling polymerization, and emulsion polymerization.

Emulsion polymerization is a biphasic process that typically occurs in either an oil-in-water (o/w) or water-in-oil (w/o) system.<sup>107</sup> In emulsion polymerization, monomer droplets are mechanically dispersed in a continuous phase of surfactant

and initiator.<sup>108</sup> The initiator penetrates these droplets and reacts with monomers to form spherical polymer particles.

In Pickering emulsion polymerization, the dispersion system is stabilized by small solid particles that adhered to the surface of monomer droplets.<sup>109</sup> A crucial step in Pickering emulsion polymerization is the formation of stable Pickering emulsion, which makes the nanoparticles choice pivotal. Various solid particles, such as calcium carbonate and barium sulfate,<sup>110</sup> clays,<sup>111-112</sup> carbon black,<sup>113</sup> carbon nanotubes,<sup>114</sup> magnetic particles,<sup>114-115</sup> silica nanoparticles<sup>116-118</sup> and metal–organic framework,<sup>119</sup> have been employed to prepare Pickering emulsions. Hydrophobic particles stabilize oil-in-water and hydrophilic particles stabilize water-in-oil emulsions, respectively.<sup>120</sup>

Pickering emulsion polymerization offers several advantages, such as simplicity, high polymer yields, and precise control over the final particle size. These characteristics render Pickering emulsion polymerization a promising method for preparing desired MIPs. Silica nanoparticles and attapulgite-coupled magnetic nanoparticles have been extensively employed for fabricating MIP microspheres for various applications, ranging from binding  $\beta$ -receptor blocker drugs, proteins, and steroids to  $\lambda$ -cyhalothrin.

To enhance the accessibility of MIP recognition sites, our group proposed using template molecules bonded to silica nanoparticles as a stabilizer to form Pickering emulsions. After polymerization, the silica nanoparticles could be removed using a hydrofluoric acid solution, to produce a permeable layer wherein all the binding sites are on the MIP surface.

In paper IV, we described the use of a DFNS structure containing 20 nm pores for immobilizing Hb for the subsequent Pickering emulsion polymerization. As shown in Figure 16, Hb-coated DFNS was first used to stabilize an oil-in-water emulsion comprising functional and crosslinking monomers in the oil phase. After the FRP of the oil phase, Hb and DFNS were removed to leave Hb-imprinted cavities on the polymer surface.

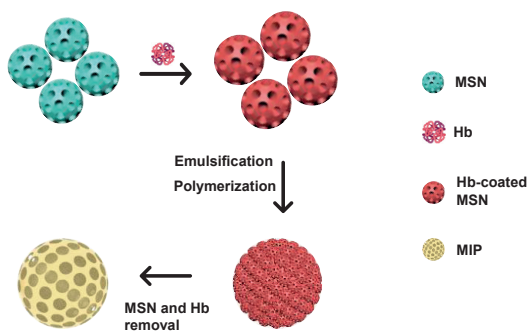


**Figure 16.** Schematic of MIP preparation *via* Pickering emulsion polymerization.

Figure 17 shows that the DFNS displayed the highest Hb-loading capacity compared to Hb loadings on nonporous silica nanoparticles synthesized using the one-step Stöber procedure [BET surface area: 17 m<sup>2</sup>/g; particle diameter: ~250 nm (by DLS)] and porous silica purchased from Sigma–Aldrich [surface area 590–690 m<sup>2</sup>/g; size 5–20 nm (by TEM)], which indicated that the high surface area and dendritic pore structure of DFNS increase protein loading. Additionally, the use of DFNS further increased the number of imprinted binding sites because the Hb loading capacity of this MIP was higher than that of the MIP reported in a previous study in which porous silica purchased from Sigma–Aldrich was used as the stabilizer.<sup>121</sup>

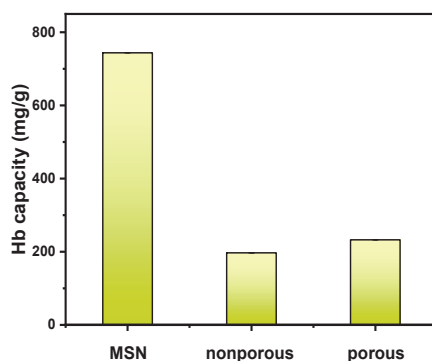


**Figure 17.** Hb-loading capacities of different nanosilicas.

## 4.2 Covalent imprinting based on boronate affinity

Wulff pioneered covalent imprinting,<sup>122–123</sup> in which functional monomers form complexes with template molecules *via* reversible covalent bonds (such as boronic ester), prior to polymerization, and during subsequent rebinding. Owing to the stability of covalent interactions, covalent imprinting enables the generation of more uniformly distributed binding sites. Furthermore, the structures of guest-binding sites are better understood in covalent imprinting.

Covalent molecular imprinting is mainly conducted using two facile and widely applicable boronate affinity-based approaches. In one approach, especially for small molecules, the template is first mixed with the monomer in an alkaline solution containing an appropriate porogen (pH ≥ 8.0), and the template and monomer form covalent complexes *via* boronate affinity, which drives molecular self-assembly. Then, the complexes are mixed with the crosslinker and initiators, and radical polymerization is initiated to obtain MIPs. In Paper II, ARS and 4-

vinylphenylboronic acid were used as the template and functional monomer, respectively. First, ARS was mixed with VPBA in an ethanol-containing phosphate buffer (pH 8.5) solution. Then, the complexes were mixed with the crosslinker (N,N-methylenebis(acrylamide)) and redox initiator (ammonium persulfate/N,N,N',N'-tetramethylethylenediamine) to initiate the polymerization and to form the MIPs (Figure 18).

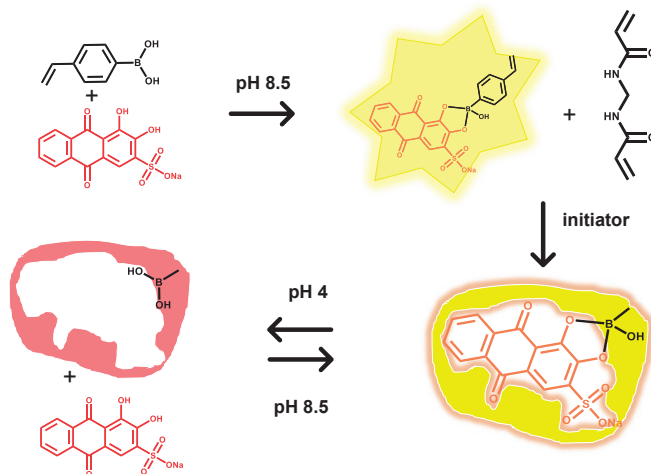


**Figure 18.** Synthesis of ARS-imprinted polymer particles.

Because the formation of the ARS–VPBA complex generates strong fluorescence emission, the status of the template binding can be monitored throughout the entire reaction in real time. This crucial aspect facilitates a deeper understanding of imprinting process. Figure 19a shows the change in the fluorescence spectrum of the polymerization mixture after the imprinting reaction started at 40 °C. The change in the fluorescence intensity of the reaction mixture (at 630 nm) is shown in Figure 19b. In the first 10 min, the fluorescence intensified, presumably because the molecular motion of the boronic acid–ARS complex reduced when the functional monomer was linked to growing oligomers. After 10 min of polymerization, the fluorescence started to weaken until it became constant. The weakened fluorescence may be attributed to light scattering by emerging insoluble particles. In addition, the maximum emission wavelength shifted from 620 to 640 nm within the first 20 min of polymerization (Figure 19c), which suggests that the boronic acid-bound ARS increasingly formed dimers or aggregated structures at imprinted sites. Within the first 20 min of the reaction, the fluorescence wavelength and intensity both varied, which agree with the findings of a previous study,<sup>124</sup> and confirms that particles nucleated and molecular-binding sites formed in early imprinting stages.

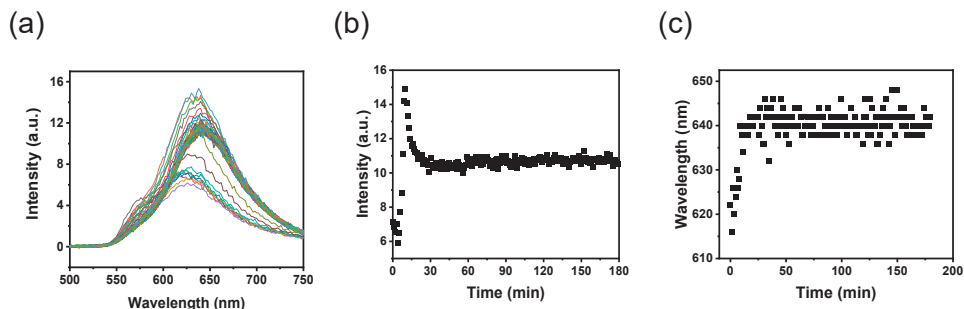


**Figure 19.** (a) Fluorescence spectra measured at different times for reaction mixture used to prepare ARS-imprinted polymer. (b) Changes in fluorescence intensity at 630 nm with increasing polymerization time. (c) Changes in maximum emission wavelength with increasing polymerization time.

Boronate affinity-based controllable oriented surface imprinting is another approach for imprinting.<sup>125-126</sup> As shown in Figure 20, a glycoprotein template is first immobilized on a boronic acid-functionalized substrate surface *via* boronate affinity binding. Then, a thin polymer film is deposited around the immobilized glycoprotein. After the glycoprotein is removed, cavity that complement the molecular shape of the template is generated in the imprinting layer. In certain cases, the use of only a boronic acid functional monomer may not provide sufficient selectivity owing to competing *cis*-diol containing biomolecules.<sup>127-128</sup> To address this issues, additional functional monomers, such as polymerizable pyrrolidyl acrylate and 2-methacryloyloxyethyl phosphorylcholine are employed.<sup>128</sup> The pyrrolidyl group interacts with the protein molecule *via* electrostatic interactions, while the phosphorylcholine group enhances biocompatibility and reduces nonspecific protein adsorption. Controlled/living radical polymerization is used to control the polymer film's thickness. In another approach, a thin film is grafted by polycondensing ethoxysilane derivatives that can interact with a specially derivatized C-terminal nonapeptide epitope.<sup>129-130</sup> The resulting MIPs can bind both the full protein and the exposed peptide epitope. To avoid the use of polymerization initiators and organic solvents that can denature proteins, pattern-imprinted boronic acid-centered self-assembled monolayers (SAMs) have previously been suggested as an alternative to MIP films. One example involves a SAM containing a 1,2-dithiolane derivative, which offers additional binding sites and improved stability through H-bonding and an oligo(ethylene glycol) moiety to reduce nonspecific protein binding.<sup>131</sup> Another SAM bearing an orthogonally functionalized acrylamide–alkyne cysteine derivative has previously been synthesized for surface imprinting.<sup>132</sup> The phenylboronic acid groups were grafted on the imprinted pattern *via* copolymerization to provide high stability, and the residual alkyne functionality was capped off to form an ordered pocket around the immobilized glycoprotein template.

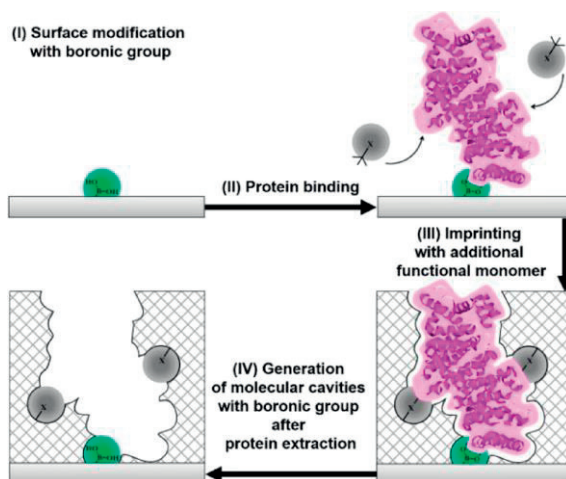


**Figure 20.** Schematic showing protein imprinting on boronic acid-functionalized surface. Reprinted with permission from reference 125. Copyright 2020 American Chemical Society.

### 4.3 DNA in molecular imprinting and sensing

With technological advances, DNA fragments have become programmable and easily modifiable. To improve signaling and binding affinity, DNA oligonucleotides have started to be used. Owing to their specific molecular recognition capabilities, DNA aptamers can improve the binding affinity of MIPs. Additionally, the polymer matrices can incorporate DNA sequences or structures, which enables DNA sequences with low binding affinity to be rescued through imprinting. DNA can be easily modified using various functional groups, such as acrydite, thiolate, biotin, or fluorophores, which enable bioconjugation and signal transduction.<sup>133-134</sup>

Spivak et al. used two acrydite-modified aptamers that could bind to different positions in thrombin to form a sandwich-like complex.<sup>135</sup> The aptamer–thrombin–aptamer complex was then imprinted in a bulk hydrogel with a few acrylic monomers. After the thrombin was removed, the MIP hydrogel exhibited a reversible volumetric change in response to thrombin. The imprinting factor of the aptamer–MIP hydrogel was much higher than that of the plain MIP hydrogel which suggested the importance of the aptamers. Liu et al. immobilized aptamers on a gold-coated substrate through a thiol–gold bond. The controlled dopamine polymerization around aptamer-anchored proteins entrapped the proteins, which were then removed to obtain MIPs. The authors confirmed that the aptamer at the bottom of the molecular cavities played a vital role in the selectivity of the resulting MIPs.<sup>136</sup> Liu et al. exploited both noncovalent and covalent binding properties of boronic acid and copolymerized it with the adenosine aptamer to prepare MIPs.

Compared with the boronic acid-free aptamer–MIPs, the boronic acid-containing aptamer–MIP copolymer exhibited 115-fold and 230-fold higher selectivity for adenosine against deoxyadenosine at pH 6.4 and against cytidine, respectively.<sup>137</sup>

Additionally, DNA has previously been combined with luminescence/fluorescence nanoparticles and quantum dots for signaling MIPs binding. Li et al. immobilized enrofloxacin (ENR)-specific aptamer on luminescent upconversion nanoparticles (UCNPs).<sup>138</sup> The immobilized aptamers were bound with ENR to produce a “pre-polymerization” complex for the subsequent nanoparticle formation. Then, the ENR was removed to generate luminescent hybrid MIPs. When the hybrid MIPs were rebound to the target, an energy-transfer system was formed between the UCNPs and target, which weakened the fluorescence emission. The ENR concentration was proportional to the decrease in the luminescence intensity over the range of 0.5 – 10 ng/mL and the limit of detection and quantification were 0.04 and 0.12 ng/mL, respectively. Yong et al. utilized quantum dot (QD) supports, a thiol-modified aptamer and methacrylic acid as functional monomers, and kanamycin as a template to prepare QD-MIPs.<sup>139</sup> Owing to the enhanced aptamer-induced adsorptive affinity, the fluorescence intensified when the QD-MIPs were rebound to kanamycin target. The fluorescence linearly intensified with increasing kanamycin concentration in the range from 0.05 to 10.0 µg/mL and the limit of detection was 0.013 µg/mL.

In Paper IV, DNA was used to amplify the molecular recognition signal in MIPs. Thiol-functionalized ssDNA was conjugated to the captured Hb (via its cysteine residue) *in situ*. Then, MIP–Hb–ssDNA functioned as an initiator to trigger the HCR between two hairpin DNA strands that were labeled with fluorophores and quenchers. The HCR reaction opened the hairpin structure to form nicked dsDNA and generated fluorescence emission concomitantly (Figure 21). The linear relationship between fluorescence intensity and the logarithm Hb concentration in the range of 0.01–1 mg/mL was obtained. The limit of Hb detection was as low as 6 µg/mL.

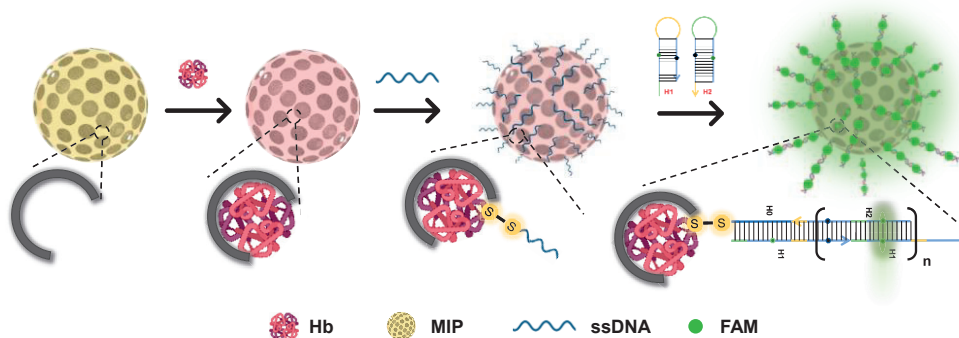


**Figure 21.** Combination of MIP with HCR for high-sensitivity Hb detection.

# Chapter 5 Conclusion and future outlooks

We designed and developed molecular recognition materials based on BA, DNA, and MIPs, which offer cost-effective solutions with high specificity and affinity for bioanalytical applications.

In Paper I, we delved into the application of the CuAAC click reaction and intermediate polymer brushes, pNIPAm-*co*-pGMA, for effectively immobilizing BA in DFNS nanopores. Our approach involved the synthesis of two distinct boronate affinity materials. The first method involved the direct click conjugation of phenylboronic acid on DFNS, while the second method entailed polymer chain and subsequent click conjugations. Compared with the polymer-chain-free modified DFNS, the polymer-chain-bearing modified DFNS exhibited more BAs and a superior binding capacity. Owing to nanochannel-induced size exclusion in the DFNS, both boronic acid-modified DFNS could bind small *cis*-diol molecules in the presence of large glycoproteins. After the boronic acid-modified DFNS catches target molecules from complex substitutes, we can introduce supplementary reagents to visualize the captured targets or trigger a remarkable fluorescence response signal.

Building on the synergistic potential of BA, Paper II explored the combination of BA with molecular imprinting technique. ARS and VPBA were selected as the template and functional monomer, respectively, to synthesize MIPs *via* precipitation polymerization. The template-functional monomer complex plays an important role for studying molecular imprinting and tracking the template binding status *via* real-time fluorescence measurements. In addition, MIPs can be used as a recyclable sensor to detect Cu<sup>2+</sup> ions without any tedious sample preparation. With guidance obtained from a deep understanding of molecular imprinting, MIP particles that exhibit improved selectivity and sensitivity will be developed.

Paper III described a “turn-on” fluorescence biosensor developed based on the FAM-ssDNA/DFNS@DA complex for rapidly and straightforwardly detecting nucleic acid sequences. The combination of the unique DFNS structure and PDA-coating-induced fluorescence quenching enabled the construction of a fluorescence sensor that can tolerate various interfering molecules in biological samples. The release of the fluorophore-labeled ssDNA upon target recognition leads to effective

fluorescence recovery, which enables the rapid and specific detection of nucleic acid targets. Future work could introduce DNA amplification methods to enhance the sensitivity of the biosensor.

Paper IV described how DNA was used to signal MIPs binding. Hb-MIPs were synthesized using Pickering emulsion polymerization, wherein DFNS and Hb functioned as the stabilizer and template, respectively. DFNS has a higher capacity for Hb than other silica nanoparticles, which improved the capacity and selectivity of the Hb-MIPs. The HCR was employed to amplify the MIP-induced Hb recognition and generated a more easily detectable fluorescence signal. This MIP-based, nucleic acid-amplified strategy enabled the establishment of a linear relationship between the fluorescence intensity and logarithmic Hb concentration in the range of 0.01–1 mg/mL. Future work will focus on optimizing the MIP synthesis to obtain nano-MIPs and enhance both the selectivity and sensitivity. Additionally, the strategy of using DNA to signal MIPs binding can be integrated with a 96 well plate reader to achieve high-throughput detection.

Overall, the thesis represents an important contribution to molecular recognition materials. The integration of BA, DNA, and MIPs has opened doors for cost-effective, specific, and sensitive molecular detection. Furthermore, the introduction of fluorescent reagents to signal recognition events has led to more easily detectable fluorescence signals. These advancements promise exciting prospects for advancing bioanalytical sciences and have excellent potential for practical applications in diverse fields.

# Acknowledgements

Time has flown by, and I am filled with a mix of emotions as I reflect on my four-year journey in Lund. I have experienced both setbacks and failures, which have taught me valuable lessons, as well as successes in experiments that have brought a sense of achievement. Amidst the confusion and uncertainty, I have also found moments of clarity and relief. I am incredibly fortunate to have exceptional colleagues and supportive friends who have provided care and assistance, always inspiring me to move forward with courage and helping me complete my studies successfully. To each of them, I extend my heartfelt gratitude and best wishes.

First and foremost, I am deeply grateful to my supervisor, Prof. Lei Ye, for your unwavering support and guidance throughout my academic journey. You have been a mentor in my studies, as well as a source of care and selfless assistance in my personal life. Your encouragement has propelled me to overcome challenges, and your teachings have shaped my understanding of professionalism. I have gained immense knowledge from your expertise, rigorous scholarship, eloquent writing, humble and approachable nature, and your positive and optimistic outlook. You are a true role model for my lifelong pursuit of learning.

To my co-supervisor, Dr. Solmaz Hajizadeh, thank you for engaging in insightful discussions and for supporting both my scientific and non-scientific endeavors. Thank you for providing comfort and encouragement, as well as for maintaining the organization and efficiency of our laboratory.

To Dr. Cedric Dicko, thank you for your assistance with the measurement of fluorescence lifetime curves and troubleshooting during the experiments. Your humor and knowledge have made the research process more enjoyable.

To Prof. Per-Olof Larsson, thank you for your invaluable assistance in designing and conducting the fluorescent microscopy experiment. Your expertise has been essential to the success of my research.

To Dr. Helena Persson, thank you for your guidance in detecting miR-21 in cancer cells and resolving experimental issues. Your insights have been invaluable to my work.

I am grateful to all past and present members of my research group, including Hongwei Zheng, Pengfei Guo, Haiyue Gong, Onibag Gutierrez Artilles, Man Zhang, Hainan Zeng, Pian Wu, Zeeshan Ali, Supicha Kachenton, Thi Hoai Thu Trinh,

Qicheng Zhang, Erum Ayub, Lia Perez, and Pannawich Thirabowonkitphithan. The time we spent together, both within and outside the laboratory, holds cherished memories. I am grateful for your friendship, support, and collaboration.

To Prof. Leif Bülow, Liselotte Andersson, Dr. Johan Svensson Bonde, Dr. Lieselotte Cloetens, Dr. Sofia Marmon, Dr. Jose Zambrano, Dr. Mona-Lissa-Khaled Halablab, Pamela Soto Garcia, Juanita Francis, Simon Christensen, Leonard Growth, Karin Kettisen, and all other colleagues in Tillämpad Biokemi, I express my utmost gratitude for your assistance and support. Thank you for creating a wonderful environment and for the memorable times we shared in the division. Our department is a warm and welcoming place, and I feel privileged to be part of this extensive family. I will miss the laughter at the Christmas table and our excursion times.

To all my Chinese friends whom I had the pleasure of meeting in Lund, it has been a true joy to have you by my side during this journey. The memories we created together through funny parties and group travels have added richness and vibrancy to my life. Thank you for your friendship and support.

To Prof. Rui Lu, thank you for supervising me during my master's studies and supporting my scholarship application for doctoral position. Your guidance has been invaluable to my academic career.

Last but not least, my deepest gratitude goes to my family. To my parents, thank you for your unwavering support and love. Your sacrifices have made my wonderful and stress-free life abroad possible. To my younger sister, thank you for being there to lend an ear to my complaints. Thank you my partner, Haochen, for your support and preparing delicious and diverse meals. I am also grateful for our joint effort in creating the cover picture for this thesis.

I want to thank everyone who has cared for and helped me over the past twenty years! Your support means the world to me. In my future career, I will strive to meet your expectations, pursue my dreams, and become the best version of myself. Thank you all for believing in me.

# References

1. He, M.; Wei, Y.; Wang, R.; Wang, C.; Zhang, B.; Han, L., Boronate Affinity Magnetic Nanoparticles with Hyperbranched Polymer Brushes for the Adsorption of Cis-Diol Biomolecules. *Microchim. Acta* **2019**, 186.
2. Hansen, M. M.; Jolly, R. A.; Linder, R. J., Boronic Acids and Derivatives - Probing the Structure-Activity Relationships for Mutagenicity. *Org. Process Res. Dev.* **2015**, 19, 1507-1516.
3. Lor, J. P.; Edwards, J. O., Polyol Complexes and Structure of the Benzeneboronate Ion. *J. Org. Chem.* **1959**, 24, 769-774.
4. Nishiyabu, R.; Kubo, Y.; James, T. D.; Fossey, J. S., Boronic Acid Building Blocks: Tools for Sensing and Separation. *Chem. Commun.* **2011**, 47, 1106-1123.
5. Wu, X.; Li, Z.; Chen, X. X.; Fossey, J. S.; James, T. D.; Jiang, Y. B., Selective Sensing of Saccharides Using Simple Boronic Acids and Their Aggregates. *Chem. Soc. Rev.* **2013**, 42, 8032-8048.
6. Brooks, W. L. A.; Sumerlin, B. S., Synthesis and Applications of Boronic Acid-Containing Polymers: From Materials to Medicine. *Chem. Rev.* **2016**, 116, 1375-1397.
7. Potter, O. G.; Breadmore, M. C.; Hilder, E. F., Boronate Functionalised Polymer Monoliths for Microscale Affinity Chromatography. *Analyst* **2006**, 131, 1094-1096.
8. Li, D.; Li, Y.; Li, X.; Bie, Z.; Pan, X.; Zhang, Q.; Liu, Z., A High Boronate Avidity Monolithic Capillary for the Selective Enrichment of Trace Glycoproteins. *J. Chromatogr. A* **2015**, 1384, 88-96.
9. Lin, Z.; Pang, J.; Yang, H.; Cai, Z.; Zhang, L.; Chen, G., One-Pot Synthesis of an Organic-Inorganic Hybrid Affinity Monolithic Column for Specific Capture of Glycoproteins. *Chem. Commun.* **2011**, 47, 9675-9677.
10. Kong, S.; Zhang, Q.; Yang, L.; Huang, Y.; Liu, M.; Yan, G.; Zhao, H.; Wu, M.; Zhang, X.; Yang, P.; Cao, W., Effective Enrichment Strategy Using Boronic Acid-Functionalized Mesoporous Graphene-Silica Composites for Intact N- and O-Linked Glycopeptide Analysis in Human Serum. *Anal. Chem.* **2021**, 93, 6682-6691.
11. Feng, J.; She, X.; He, X.; Zhu, J.; Li, Y.; Deng, C., Synthesis of Magnetic Graphene/Mesoporous Silica Composites with Boronic Acid-Functionalized Pore-Walls for Selective and Efficient Residue Analysis of Aminoglycosides in Milk. *Food Chem.* **2018**, 239, 612-621.

12. Halbus, A. F.; Horozov, T. S.; Paunov, V. N., Strongly Enhanced Antibacterial Action of Copper Oxide Nanoparticles with Boronic Acid Surface Functionality. *ACS Appl. Mater. Interfaces* **2019**, *11*, 12232-12243.
13. Frasconi, M.; Tel-Vered, R.; Riskin, M.; Willner, I., Surface Plasmon Resonance Analysis of Antibiotics Using Imprinted Boronic Acid-Functionalized Au Nanoparticle Composites. *Anal. Chem.* **2010**, *82*, 2512-2519.
14. Nazemi, S. A.; Olesińska, M.; Pezzella, C.; Varriale, S.; Lin, C. W.; Corvini, P. F. X.; Shahgaldian, P., Immobilisation and Stabilisation of Glycosylated Enzymes on Boronic Acid-Functionalised Silica Nanoparticles. *Chem. Commun.* **2021**, *57*, 11960-11963.
15. Awino, J. K.; Gunasekara, R. W.; Zhao, Y., Selective Recognition of D-Aldohexoses in Water by Boronic Acid-Functionalized, Molecularly Imprinted Cross-Linked Micelles. *J. Am. Chem. Soc.* **2016**, *138*, 9759-9762.
16. Manju, S.; Hari, P. R.; Sreenivasan, K., Fluorescent Molecularly Imprinted Polymer Film Binds Glucose with a Concomitant Changes in Fluorescence. *Biosens. Bioelectron.* **2010**, *26*, 894-897.
17. Chen, W.; Guo, Z.; Yu, H.; Liu, Q.; Fu, M., Molecularly Imprinted Colloidal Array with Multi-Boronic Acid Sites for Glycoprotein Detection under Neutral Ph. *J. Colloid Interface Sci.* **2022**, *607*, 1163-1172.
18. Chen, Y.; Tong, J.; Dong, J.; Luo, J.; Liu, X., A Temperature-Responsive Boronate Core Cross-Linked Star (Ccs) Polymer for Fast and Highly Efficient Enrichment of Glycoproteins. *Small* **2019**, *15*.
19. Bapat, A. P.; Roy, D.; Ray, J. G.; Savin, D. A.; Sumerlin, B. S., Dynamic-Covalent Macromolecular Stars with Boronic Ester Linkages. *J. Am. Chem. Soc.* **2011**, *133*, 19832-19838.
20. Wang, Y.; Du, X.; Liu, Z.; Shi, S.; Lv, H., Dendritic Fibrous Nano-Particles (Dfnps): Rising Stars of Mesoporous Materials. *J. Mater. Chem. A* **2019**, *7*, 5111-5152.
21. Kresge, C. T.; Leonowicz, M. E.; Roth, W. J.; Vartuli, J. C.; Beck, J. S., Ordered Mesoporous Molecular Sieves Synthesized by a Liquid-Crystal Template Mechanism. *Nature* **1992**, *359*, 710-712.
22. Zhao, D.; Feng, J.; Huo, Q.; Melosh, N.; Fredrickson, G. H.; Chmelka, B. F.; Stucky, G. D., Triblock Copolymer Syntheses of Mesoporous Silica with Periodic 50 to 300 Angstrom Pores. *Science* **1998**, *279*, 548-52.
23. Polshettiwar, V.; Cha, D.; Zhang, X.; Basset, J. M., High-Surface-Area Silica Nanospheres (Kcc-1) with a Fibrous Morphology. *Angew. Chem. Int. Ed.* **2010**, *49*, 9652-9656.
24. Du, X.; He, J., Fine-Tuning of Silica Nanosphere Structure by Simple Regulation of the Volume Ratio of Cosolvents. *Langmuir* **2010**, *26*, 10057-10062.
25. Park, D. S.; Yun, D.; Kim, T. Y.; Baek, J.; Yun, Y. S.; Yi, J., A Mesoporous Carbon-Supported Pt Nanocatalyst for the Conversion of Lignocellulose to Sugar Alcohols. *ChemSusChem* **2013**, *6*, 2281-2289.

26. Li, X.; Chen, X.; Miao, G.; Liu, H.; Mao, C.; Yuan, G.; Liang, Q.; Shen, X.; Ning, C.; Fu, X., Synthesis of Radial Mesoporous Bioactive Glass Particles to Deliver Osteoactivin Gene. *J. Mater. Chem. B* **2014**, *2*, 7045-7054.
27. Shen, D.; Yang, J.; Li, X.; Zhou, L.; Zhang, R.; Li, W.; Chen, L.; Wang, R.; Zhang, F.; Zhao, D., Biphasic Stratification Approach to Three-Dimensional Dendritic Biodegradable Mesoporous Silica Nanospheres. *Nano Lett.* **2014**, *14*, 923-932.
28. Yang, Y.; Bernardi, S.; Song, H.; Zhang, J.; Yu, M.; Reid, J. C.; Strounina, E.; Searles, D. J.; Yu, C., Anion Assisted Synthesis of Large Pore Hollow Dendritic Mesoporous Organosilica Nanoparticles: Understanding the Composition Gradient. *Chem. Mater.* **2016**, *28*, 704-707.
29. Bayal, N.; Singh, R.; Polshettiwar, V., Nanostructured Silica–Titania Hybrid Using Dendritic Fibrous Nanosilica as a Photocatalyst. *ChemSusChem* **2017**, *10*, 2182-2191.
30. Milner, S. T., Polymer Brushes. *Science* **1991**, *251*, 905-14.
31. Barbey, R.; Lavanant, L.; Paripovic, D.; Schüwer, N.; Sugnaux, C.; Tugulu, S.; Klok, H. A., Polymer Brushes Via Surface-Initiated Controlled Radical Polymerization: Synthesis, Characterization, Properties, and Applications. *Chem. Rev.* **2009**, *109*, 5437-527.
32. Zhao, B.; Brittain, W. J., Polymer Brushes: Surface-Immobilized Macromolecules. *Prog. Polym. Sci.* **2000**, *25*, 677-710.
33. Hucknall, A.; Rangarajan, S.; Chilkoti, A., In Pursuit of Zero: Polymer Brushes That Resist the Adsorption of Proteins. *Adv. Mater.* **2009**, *21*, 2441-2446.
34. Vana, P., *Controlled Radical Polymerization at and from Solid Surfaces*. Springer: 2016.
35. Andersson, J.; Järleback, J.; Kk, S.; Schaefer, A.; Hailes, R.; Palasingh, C.; Santoso, B.; Vu, V.-T.; Huang, C.-J.; Westerlund, F.; Dahlin, A., Polymer Brushes on Silica Nanostructures Prepared by Aminopropylsilatrane Click Chemistry: Superior Antifouling and Biofunctionality. *ACS Appl. Mater. Interfaces* **2023**, *15*, 10228-10239.
36. Leitner, N. S.; Schroffenegger, M.; Reimhult, E., Polymer Brush-Grafted Nanoparticles Preferentially Interact with Opsonins and Albumin. *ACS Appl. Bio Mater.* **2021**, *4*, 795-806.
37. Nagase, K.; Ishii, S.; Takeuchi, A.; Kanazawa, H., Temperature-Modulated Antibody Drug Separation Using Thermoresponsive Mixed Polymer Brush-Modified Stationary Phase. *Sep. Purif. Technol.* **2022**, *299*, 121750.
38. Zheng, S. Y.; Ni, Y.; Zhou, J.; Gu, Y.; Wang, Y.; Yuan, J.; Wang, X.; Zhang, D.; Liu, S.; Yang, J., Photo-Switchable Supramolecular Comb-Like Polymer Brush Based on Host-Guest Recognition for Use as Antimicrobial Smart Surface. *J. Mater. Chem. B* **2022**, *10*, 3039-3047.
39. Springsteen, G.; Wang, B., Alizarin Red S. As a General Optical Reporter for Studying the Binding of Boronic Acids with Carbohydrates. *Chem. Commun.* **2001**, 1608-1609.
40. Xu, Z.; Uddin, K. M. A.; Kamra, T.; Schnadt, J.; Ye, L., Fluorescent Boronic Acid Polymer Grafted on Silica Particles for Affinity Separation of Saccharides. *ACS Appl. Mater. Interfaces* **2014**, *6*, 1406-1414.

41. Palit, D. K.; Pal, H.; Mukherjee, T.; Mittal, J. P., Photodynamics of the S1 State of Some Hydroxy- and Amino-Substituted Naphthoquinones and Anthraquinones. *Journal of the Chemical Society, Faraday Transactions* **1990**, *86*, 3861-3869.
42. Schumacher, S.; Nagel, T.; Scheller, F. W.; Gajovic-Eichelmann, N., Alizarin Red S as an Electrochemical Indicator for Saccharide Recognition. *Electrochim. Acta* **2011**, *56*, 6607-6611.
43. Lee, S. H.; Gupta, M. K.; Bang, J. B.; Bae, H.; Sung, H. J., Current Progress in Reactive Oxygen Species (Ros)-Responsive Materials for Biomedical Applications. *Adv. Healthc. Mater.* **2013**, *2*, 908-915.
44. Kuivila, H. G.; Armour, A. G., Electrophilic Displacement Reactions. Ix. Effects of Substituents on Rates of Reactions between Hydrogen Peroxide and Benzeneboronic Acid1-3. *J. Am. Chem. Soc.* **1957**, *79*, 5659-5662.
45. Patenall, B. L.; Williams‡, G. T.; Gwynne, L.; Stephens, L. J.; Lampard, E. V.; Hathaway, H. J.; Thet, N. T.; Young, A. E.; Sutton, M. J.; Short, R. D.; Bull, S. D.; James, T. D.; Sedgwick, A. C.; Jenkins, A. T. A., Reaction-Based Indicator Displacement Assay (Ria) for the Development of a Triggered Release System Capable of Biofilm Inhibition. *Chem. Commun.* **2019**, *55*, 15129-15132.
46. Sun, X.; Lacina, K.; Ramsamy, E. C.; Flower, S. E.; Fossey, J. S.; Qian, X.; Anslyn, E. V.; Bull, S. D.; James, T. D., Reaction-Based Indicator Displacement Assay (Ria) for the Selective Colorimetric and Fluorometric Detection of Peroxynitrite. *Chem. Sci.* **2015**, *6*, 2963-2967.
47. Wang, Q.; Li, G.; Xiao, W.; Qi, H.; Li, G., Glucose-Responsive Vesicular Sensor Based on Boronic Acid–Glucose Recognition in the Ars/Pba/Dbbtac Covesicles. *Sens. Actuators B Chem.* **2006**, *119*, 695-700.
48. Ma, W. M. J.; Pereira Morais, M. P.; D’Hooge, F.; van den Elsen, J. M. H.; Cox, J. P. L.; James, T. D.; Fossey, J. S., Dye Displacement Assay for Saccharide Detection with Boronate Hydrogels. *Chem. Commun.* **2009**, 532-534.
49. Liang, X.; Bonizzoni, M., Boronic Acid-Modified Poly(Amidoamine) Dendrimers as Sugar-Sensing Materials in Water. *J. Mater. Chem. B* **2016**, *4*, 3094-3103.
50. Wang, L.-L.; Qiao, J.; Liu, H.-H.; Hao, J.; Qi, L.; Zhou, X.-P.; Li, D.; Nie, Z.-X.; Mao, L.-Q., Ratiometric Fluorescent Probe Based on Gold Nanoclusters and Alizarin Red-Boronic Acid for Monitoring Glucose in Brain Microdialysate. *Anal. Chem.* **2014**, *86*, 9758-9764.
51. Belmont, P.; Constant, J.-F.; Demeunynck, M., Nucleic Acid Conformation Diversity: From Structure to Function and Regulation. *Chem. Soc. Rev.* **2001**, *30*, 70-81.
52. Schilter, D., Translation: The Proof Is in the Protein. *Nat. Rev. Chem.* **2017**, *1*, 0011.
53. Gautam, A., Southern and Northern Blotting. In *DNA and Rna Isolation Techniques for Non-Experts*, Gautam, A., Ed. Springer International Publishing: Cham, 2022; pp 165-169.
54. Erlich, H. A., Polymerase Chain Reaction. *J. Clin. Immunol.* **1989**, *9*, 437-447.
55. Blauwkamp, T. A.; Thair, S.; Rosen, M. J.; Blair, L.; Lindner, M. S.; Vilfan, I. D.; Kawli, T.; Christians, F. C.; Venkatasubrahmanyam, S.; Wall, G. D.; Cheung, A.; Rogers,

- Z. N.; Meshulam-Simon, G.; Huijse, L.; Balakrishnan, S.; Quinn, J. V.; Hollemon, D.; Hong, D. K.; Vaughn, M. L.; Kertesz, M.; Bercovici, S.; Wilber, J. C.; Yang, S., Analytical and Clinical Validation of a Microbial Cell-Free DNA Sequencing Test for Infectious Disease. *Nat. Microbiol.* **2019**, *4*, 663-674.
56. Anzalone, A. V.; Gao, X. D.; Podracky, C. J.; Nelson, A. T.; Koblan, L. W.; Raguram, A.; Levy, J. M.; Mercer, J. A. M.; Liu, D. R., Programmable Deletion, Replacement, Integration and Inversion of Large DNA Sequences with Twin Prime Editing. *Nat. Biotechnol.* **2022**, *40*, 731-740.
57. Shahmuradyan, A.; Krull, U. J., Intrinsically Labeled Fluorescent Oligonucleotide Probes on Quantum Dots for Transduction of Nucleic Acid Hybridization. *Anal. Chem.* **2016**, *88*, 3186-3193.
58. Bhuckory, S.; Lahtinen, S.; Höysniemi, N.; Guo, J.; Qiu, X.; Soukka, T.; Hildebrandt, N., Understanding FRET in Upconversion Nanoparticle Nucleic Acid Biosensors. *Nano Lett.* **2023**, *23*, 2253-2261.
59. Lubin, A. A.; Plaxco, K. W., Folding-Based Electrochemical Biosensors: The Case for Responsive Nucleic Acid Architectures. *Acc. Chem. Res.* **2010**, *43*, 496-505.
60. Bonnet, G.; Tyagi, S.; Libchaber, A.; Kramer, F. R., Thermodynamic Basis of the Enhanced Specificity of Structured DNA Probes. *Proc. Natl. Acad. Sci. U. S. A.* **1999**, *96*, 6171-6176.
61. Tsourkas, A.; Behlke, M. A.; Rose, S. D.; Bao, G., Hybridization Kinetics and Thermodynamics of Molecular Beacons. *Nucleic Acids Res.* **2003**, *31*, 1319-30.
62. Tyagi, S.; Kramer, F. R., Molecular Beacons: Probes That Fluoresce Upon Hybridization. *Nat. Biotechnol.* **1996**, *14*, 303-308.
63. Wang, K.; Tang, Z.; Yang, C. J.; Kim, Y.; Fang, X.; Li, W.; Wu, Y.; Medley, C. D.; Cao, Z.; Li, J.; Colon, P.; Lin, H.; Tan, W., Molecular Engineering of DNA: Molecular Beacons. *Angew. Chem. Int. Ed.* **2009**, *48*, 856-870.
64. Tan, W.; Wang, K.; Drake, T. J., Molecular Beacons. *Curr. Opin. Chem. Biol.* **2004**, *8*, 547-553.
65. Huang, Q.; Chen, D.; Du, C.; Liu, Q.; Lin, S.; Liang, L.; Xu, Y.; Liao, Y.; Li, Q., Highly Multiplex PCR Assays by Coupling the 5' -Flap Endonuclease Activity of Taq DNA Polymerase and Molecular Beacon Reporters. *Proc. Natl. Acad. Sci.* **2022**, *119*, e2110672119.
66. Marras Salvatore, A. E.; Chen, L.; Shashkina, E.; Davidson Rebecca, M.; Strong, M.; Daley Charles, L.; Kreiswirth Barry, N., A Molecular-Beacon-Based Multiplex Real-Time PCR Assay to Distinguish Mycobacterium Abscessus Subspecies and Determine Macrolide Susceptibility. *J. Clin. Microbiol.* **2021**, *59*, 10.1128/jcm.00455-21.
67. Jayagopal, A.; Halfpenny, K. C.; Perez, J. W.; Wright, D. W., Hairpin DNA-Functionalized Gold Colloids for the Imaging of mRNA in Live Cells. *J. Am. Chem. Soc.* **2010**, *132*, 9789-9796.

68. Venkataraman, S.; Dirks, R. M.; Rothmund, P. W.; Winfree, E.; Pierce, N. A., An Autonomous Polymerization Motor Powered by DNA Hybridization. *Nat. Nanotechnol.* **2007**, *2*, 490-4.
69. Choi, H. M. T.; Schwarzkopf, M.; Fornace, M. E.; Acharya, A.; Artavanis, G.; Stegmaier, J.; Cunha, A.; Pierce, N. A., Third-Generation in Situ Hybridization Chain Reaction: Multiplexed, Quantitative, Sensitive, Versatile, Robust. *Development* **2018**, *145*.
70. Wu, C.; Cansiz, S.; Zhang, L.; Teng, I. T.; Qiu, L.; Li, J.; Liu, Y.; Zhou, C.; Hu, R.; Zhang, T.; Cui, C.; Cui, L.; Tan, W., A Nonenzymatic Hairpin DNA Cascade Reaction Provides High Signal Gain of Mra Imaging inside Live Cells. *J. Am. Chem. Soc.* **2015**, *137*, 4900-4903.
71. Chang, D.; Zakaria, S.; Deng, M.; Allen, N.; Tram, K.; Li, Y., Integrating Deoxyribozymes into Colorimetric Sensing Platforms. *Sensors* **2016**, *16*.
72. Keefe, A. D.; Pai, S.; Ellington, A., Aptamers as Therapeutics. *Nat. Rev. Drug Discov.* **2010**, *9*, 537-550.
73. Tuerk, C.; Gold, L., Systematic Evolution of Ligands by Exponential Enrichment: Rna Ligands to Bacteriophage T4 DNA Polymerase. *Science* **1990**, *249*, 505-510.
74. Ellington, A. D.; Szostak, J. W., In Vitro Selection of Rna Molecules That Bind Specific Ligands. *Nature* **1990**, *346*, 818-822.
75. Bunka, D. H. J.; Stockley, P. G., Aptamers Come of Age – at Last. *Nat. Rev. Microbiol.* **2006**, *4*, 588-596.
76. Tombelli, S.; Minunni, M.; Mascini, M., Analytical Applications of Aptamers. *Biosens. Bioelectron.* **2005**, *20*, 2424-2434.
77. Gotrik, M. R.; Feagin, T. A.; Csordas, A. T.; Nakamoto, M. A.; Soh, H. T., Advancements in Aptamer Discovery Technologies. *Acc. Chem. Res.* **2016**, *49*, 1903-1910.
78. McKeague, M.; Wong, R. S.; Smolke, C. D., Opportunities in the Design and Application of Rna for Gene Expression Control. *Nucleic Acids Res.* **2016**, *44*, 2987-2999.
79. Wang, B.; Zhao, C.; Wang, Z.; Yang, K.-A.; Cheng, X.; Liu, W.; Yu, W.; Lin, S.; Zhao, Y.; Cheung, K. M.; Lin, H.; Hojaiji, H.; Weiss, P. S.; Stojanović, M. N.; Tomiyama, A. J.; Andrews, A. M.; Emaminejad, S., Wearable Aptamer-Field-Effect Transistor Sensing System for Noninvasive Cortisol Monitoring. *Sci. Adv.* **2022**, *8*, eabk0967.
80. Echaide-Górriz, C.; Clément, C.; Cacho-Bailo, F.; Téllez, C.; Coronas, J., New Strategies Based on Microfluidics for the Synthesis of Metal-Organic Frameworks and Their Membranes. *J. Mater. Chem. A* **2018**, *6*, 5485-5506.
81. Katz, D. H.; Robbins, J. M.; Deng, S.; Tahir, U. A.; Bick, A. G.; Pampana, A.; Yu, Z.; Ngo, D.; Benson, M. D.; Chen, Z.-Z.; Cruz, D. E.; Shen, D.; Gao, Y.; Bouchard, C.; Sarzynski, M. A.; Correa, A.; Natarajan, P.; Wilson, J. G.; Gerszten, R. E., Proteomic Profiling Platforms Head to Head: Leveraging Genetics and Clinical Traits to Compare Aptamer- and Antibody-Based Methods. *Sci. Adv.* **2022**, *8*, eabm5164.
82. Guerrier-Takada, C.; Gardiner, K.; Marsh, T.; Pace, N.; Altman, S., The Rna Moiety of Ribonuclease P Is the Catalytic Subunit of the Enzyme. *Cell* **1983**, *35*, 849-857.

83. Breaker, R. R.; Joyce, G. F., A DNA Enzyme That Cleaves Rna. *Chem. Biol.* **1994**, *1*, 223-229.
84. Li, J.; Wu, H.; Yan, Y.; Yuan, T.; Shu, Y.; Gao, X.; Zhang, L.; Li, S.; Ding, S.; Cheng, W., Zippered G-Quadruplex/Hemin Dnazyme: Exceptional Catalyst for Universal Bioanalytical Applications. *Nucleic Acids Res.* **2021**, *49*, 13031-13044.
85. Wang, W.; Satyavolu, N. S. R.; Wu, Z.; Zhang, J. R.; Zhu, J. J.; Lu, Y., Near-Infrared Photothermally Activated Dnazyme–Gold Nanoshells for Imaging Metal Ions in Living Cells. *Angew. Chem. Int. Ed.* **2017**, *56*, 6798-6802.
86. Wu, N.; Willner, I., Dnazyme-Controlled Cleavage of Dimer and Trimer Origami Tiles. *Nano Lett.* **2016**, *16*, 2867-2872.
87. Hu, Y.; Cecconello, A.; Idili, A.; Ricci, F.; Willner, I., Triplex DNA Nanostructures: From Basic Properties to Applications. *Angew. Chem. Int. Ed.* **2017**, *56*, 15210-15233.
88. Vasquez, K. M.; Glazer, P. M., Triplex-Forming Oligonucleotides: Principles and Applications. *Q. Rev. Biophys.* **2002**, *35*, 89-107.
89. Du, Y.; Guo, S.; Dong, S.; Wang, E., An Integrated Sensing System for Detection of DNA Using New Parallel-Motif DNA Triplex System and Graphene–Mesoporous Silica–Gold Nanoparticle Hybrids. *Biomaterials* **2011**, *32*, 8584-8592.
90. Patterson, A.; Caprio, F.; Vallée-Bélisle, A.; Moscone, D.; Plaxco, K. W.; Palleschi, G.; Ricci, F., Using Triplex-Forming Oligonucleotide Probes for the Reagentless, Electrochemical Detection of Double-Stranded DNA. *Anal. Chem.* **2010**, *82*, 9109-9115.
91. Vallée-Bélisle, A.; Ricci, F.; Plaxco, K. W., Thermodynamic Basis for the Optimization of Binding-Induced Biomolecular Switches and Structure-Switching Biosensors. *Proc. Natl. Acad. Sci.* **2009**, *106*, 13802-13807.
92. Tsourkas, A.; Behlke, M. A.; Bao, G., Structure – Function Relationships of Shared - Stem and Conventional Molecular Beacons. *Nucleic Acids Res.* **2002**, *30*, 4208-4215.
93. Zhao, N.; Yan, L.; Zhao, X.; Chen, X.; Li, A.; Zheng, D.; Zhou, X.; Dai, X.; Xu, F. J., Versatile Types of Organic/Inorganic Nanohybrids: From Strategic Design to Biomedical Applications. *Chem. Rev.* **2019**, *119*, 1666-1762.
94. Shin, T. H.; Choi, Y.; Kim, S.; Cheon, J., Recent Advances in Magnetic Nanoparticle-Based Multi-Modal Imaging. *Chem. Soc. Rev.* **2015**, *44*, 4501-16.
95. Pfeffer, S. R.; Yang, C. H.; Pfeffer, L. M., The Role of Mir-21 in Cancer. *Drug Dev. Res.* **2015**, *76*, 270-277.
96. Persson, H.; Sökilde, R.; Häkkinen, J.; Pirona, A. C.; Vallon-Christersson, J.; Kvist, A.; Mertens, F.; Borg, Å.; Mitelman, F.; Höglund, M.; Rovira, C., Frequent Mirna-Convergent Fusion Gene Events in Breast Cancer. *Nat. Commun.* **2017**, *8*, 788.
97. Ye, L.; Mosbach, K., Molecular Imprinting: Synthetic Materials as Substitutes for Biological Antibodies and Receptors. *Chem. Mater.* **2008**, *20*, 859-868.

98. Cai, G.; Yu, Z.; Tang, D., Actuating Photoelectrochemical Sensing Sensitivity Coupling Core-Core-Shell Fe<sub>3</sub>O<sub>4</sub>@C@TiO<sub>2</sub> with Molecularly Imprinted Polypyrrole. *Talanta* **2020**, *219*, 121341.
99. Takeuchi, T.; Mori, T.; Kuwahara, A.; Ohta, T.; Oshita, A.; Sunayama, H.; Kitayama, Y.; Ooya, T., Conjugated-Protein Mimics with Molecularly Imprinted Reconstructible and Transformable Regions That Are Assembled Using Space-Filling Prosthetic Groups. *Angew. Chem. Int. Ed.* **2014**, *53*, 12765-12770.
100. Chianella, I.; Guerreiro, A.; Moczko, E.; Caygill, J. S.; Piletska, E. V.; De Vargas Sansalvador, I. M. P.; Whitcombe, M. J.; Piletsky, S. A., Direct Replacement of Antibodies with Molecularly Imprinted Polymer Nanoparticles in Elisa—Development of a Novel Assay for Vancomycin. *Anal. Chem.* **2013**, *85*, 8462-8468.
101. Muhammad, P.; Tu, X.; Liu, J.; Wang, Y.; Liu, Z., Molecularly Imprinted Plasmonic Substrates for Specific and Ultrasensitive Immunoassay of Trace Glycoproteins in Biological Samples. *ACS Appl. Mater. Interfaces* **2017**, *9*, 12082-12091.
102. Mosbach, K., Molecular Imprinting. *Trends Biochem. Sci.* **1994**, *19*, 9-14.
103. Ekberg, B.; Mosbach, K., Molecular Imprinting: A Technique for Producing Specific Separation Materials. *Trends Biotechnol.* **1989**, *7*, 92-96.
104. Arabi, M.; Ostovan, A.; Li, J.; Wang, X.; Zhang, Z.; Choo, J.; Chen, L., Molecular Imprinting: Green Perspectives and Strategies. *Adv. Mater.* **2021**, *33*, 2100543.
105. Pérez, N.; Whitcombe, M. J.; Vulfson, E. N., Molecularly Imprinted Nanoparticles Prepared by Core-Shell Emulsion Polymerization. *J. Appl. Polym. Sci.* **2000**, *77*, 1851-1859.
106. Gao, D.; Zhang, Z.; Wu, M.; Xie, C.; Guan, G.; Wang, D., A Surface Functional Monomer-Directing Strategy for Highly Dense Imprinting of Tnt at Surface of Silica Nanoparticles. *J. Am. Chem. Soc.* **2007**, *129*, 7859-7866.
107. Lovell, P. A.; Schork, F. J., Fundamentals of Emulsion Polymerization. *Biomacromolecules* **2020**, *21*, 4396-4441.
108. Jenjob, R.; Phakkeeree, T.; Seidi, F.; Theerasilp, M.; Crespy, D., Emulsion Techniques for the Production of Pharmacological Nanoparticles. *Macromol. Biosci.* **2019**, *19*, e1900063.
109. Spencer Umfreville, P., Cxcvi.—Emulsions. *J. Chem. Soc., Trans.* **1907**, *91*, 2001-2021.
110. Levine, S.; Sanford, E., Stabilisation of Emulsion Droplets by Fine Powders. *Can. J. Chem. Eng.* **1985**, *63*, 258-268.
111. Abend, S.; Lagaly, G., Bentonite and Double Hydroxides as Emulsifying Agents. *Clay Miner.* **2001**, *36*, 557-570.
112. Ashby, N. P.; Binks, B. P., Pickering Emulsions Stabilised by Laponite Clay Particles. *Phys. Chem. Chem. Phys.* **2000**, *2*, 5640-5646.
113. Gelot, A.; Friesen, W.; Hamza, H. A., Emulsification of Oil and Water in the Presence of Finely Divided Solids and Surface-Active Agents. *Colloids Surf.* **1984**, *12*, 271-303.

114. Wang, H.; Hobbie, E. K., Amphiphobic Carbon Nanotubes as Macroemulsion Surfactants. *Langmuir* **2003**, *19*, 3091-3093.
115. Zhou, J.; Qiao, X.; Binks, B. P.; Sun, K.; Bai, M.; Li, Y.; Liu, Y., Magnetic Pickering Emulsions Stabilized by Fe<sub>3</sub>O<sub>4</sub> Nanoparticles. *Langmuir* **2011**, *27*, 3308-3316.
116. Shen, X.; Ye, L., Interfacial Molecular Imprinting in Nanoparticle-Stabilized Emulsions. *Macromolecules* **2011**, *44*, 5631-5637.
117. Shen, X.; Xu, C.; Ye, L., Imprinted Polymer Beads Enabling Direct and Selective Molecular Separation in Water. *Soft Matter* **2012**, *8*, 7169-7176.
118. Zhou, T.; Shen, X.; Chaudhary, S.; Ye, L., Molecularly Imprinted Polymer Beads Prepared by Pickering Emulsion Polymerization for Steroid Recognition. *J. Appl. Polym. Sci.* **2014**, *131*.
119. Huo, J.; Marcello, M.; Garai, A.; Bradshaw, D., Mof-Polymer Composite Microcapsules Derived from Pickering Emulsions. *Adv. Mater.* **2013**, *25*, 2717-2722.
120. Chevalier, Y.; Bolzinger, M. A., Emulsions Stabilized with Solid Nanoparticles: Pickering Emulsions. *Colloids Surf. A Physicochem. Eng. Asp.* **2013**, *439*, 23-34.
121. Zhou, T.; Zhang, K.; Kamra, T.; Bülow, L.; Ye, L., Preparation of Protein Imprinted Polymer Beads by Pickering Emulsion Polymerization. *J. Mater. Chem. B* **2015**, *3*, 1254-1260.
122. Wulff, G.; Liu, J., Design of Biomimetic Catalysts by Molecular Imprinting in Synthetic Polymers: The Role of Transition State Stabilization. *Acc. Chem. Res.* **2012**, *45*, 239-247.
123. Wulff, G.; Vesper, W.; Grobe - Einsler, R.; Sarhan, A., Enzyme - Analogue Built Polymers, 4. On the Synthesis of Polymers Containing Chiral Cavities and Their Use for the Resolution of Racemates. *Macromol. Chem. Phys.* **1977**, *178*, 2799-2816.
124. Tse Sum Bui, B.; Haupt, K., Preparation and Evaluation of a Molecularly Imprinted Polymer for the Selective Recognition of Testosterone—Application to Molecularly Imprinted Sorbent Assays. *J. Mol. Recognit.* **2011**, *24*, 1123-1129.
125. Kalecki, J.; Iskierko, Z.; Cieplak, M.; Sharma, P. S., Oriented Immobilization of Protein Templates: A New Trend in Surface Imprinting. *ACS Sensors* **2020**, *5*, 3710-3720.
126. Liu, Z.; He, H., Synthesis and Applications of Boronate Affinity Materials: From Class Selectivity to Biomimetic Specificity. *Acc. Chem. Res.* **2017**, *50*, 2185-2193.
127. Morishige, T.; Takano, E.; Sunayama, H.; Kitayama, Y.; Takeuchi, T., Post-Imprinting-Modified Molecularly Imprinted Nanocavities with Two Synergetic, Orthogonal, Glycoprotein-Binding Sites to Transduce Binding Events into Fluorescence Changes. *ChemNanoMat* **2019**, *5*, 224-229.
128. Saeki, T.; Sunayama, H.; Kitayama, Y.; Takeuchi, T., Orientationally Fabricated Zwitterionic Molecularly Imprinted Nanocavities for Highly Sensitive Glycoprotein Recognition. *Langmuir* **2019**, *35*, 1320-1326.

129. Xing, R.; Ma, Y.; Wang, Y.; Wen, Y.; Liu, Z., Specific Recognition of Proteins and Peptides Via Controllable Oriented Surface Imprinting of Boronate Affinity-Anchored Epitopes. *Chem. Sci.* **2019**, *10*, 1831-1835.
130. Sun, C.; Pan, L.; Zhang, L.; Huang, J.; Yao, D.; Wang, C. Z.; Zhang, Y.; Jiang, N.; Chen, L.; Yuan, C. S., A Biomimetic Fluorescent Nanosensor Based on Imprinted Polymers Modified with Carbon Dots for Sensitive Detection of Alpha-Fetoprotein in Clinical Samples. *Analyst* **2019**, *144*, 6760-6772.
131. Zhang, X.; Du, X., Creation of Glycoprotein Imprinted Self-Assembled Monolayers with Dynamic Boronate Recognition Sites and Imprinted Cavities for Selective Glycoprotein Recognition. *Soft Matter* **2020**, *16*, 3039-3049.
132. Stephenson-Brown, A.; Acton, A. L.; Preece, J. A.; Fossey, J. S.; Mendes, P. M., Selective Glycoprotein Detection through Covalent Templating and Allosteric Click-Imprinting. *Chem. Sci.* **2015**, *6*, 5114-5119.
133. Liu, J., Oligonucleotide-Functionalized Hydrogels as Stimuli Responsive Materials and Biosensors. *Soft Matter* **2011**, *7*, 6757-6767.
134. Zhang, Z.; Liu, J., Molecular Imprinting with Functional DNA. *Small* **2019**, *15*, 1805246.
135. Bai, W.; Gariano, N. A.; Spivak, D. A., Macromolecular Amplification of Binding Response in Superaptamer Hydrogels. *J. Am. Chem. Soc.* **2013**, *135*, 6977-6984.
136. Li, W.; Zhang, Q.; Wang, Y.; Ma, Y.; Guo, Z.; Liu, Z., Controllably Prepared Aptamer-Molecularly Imprinted Polymer Hybrid for High-Specificity and High-Affinity Recognition of Target Proteins. *Anal. Chem.* **2019**, *91*, 4831-4837.
137. Li, Y.; Zhang, Z.; Liu, B.; Liu, J., Incorporation of Boronic Acid into Aptamer-Based Molecularly Imprinted Hydrogels for Highly Specific Recognition of Adenosine. *ACS Appl. Bio Mater.* **2020**, *3*, 2568-2576.
138. Liu, X.; Ren, J.; Su, L.; Gao, X.; Tang, Y.; Ma, T.; Zhu, L.; Li, J., Novel Hybrid Probe Based on Double Recognition of Aptamer-Molecularly Imprinted Polymer Grafted on Upconversion Nanoparticles for Enrofloxacin Sensing. *Biosens. Bioelectron.* **2017**, *87*, 203-208.
139. Geng, Y.; Guo, M.; Tan, J.; Huang, S.; Tang, Y.; Tan, L.; Liang, Y., A Fluorescent Molecularly Imprinted Polymer Using Aptamer as a Functional Monomer for Sensing of Kanamycin. *Sens. Actuators B Chem.* **2018**, *268*, 47-54.